Journal of Medicinal Chemistry

pubs.acs.org/jmc

Article

# Design of Negative and Positive Allosteric Modulators of the Cannabinoid $CB_2$ Receptor Derived from the Natural Product Cannabidiol

Gemma Navarro, Angel Gonzalez, Adrià Sánchez-Morales, Nil Casajuana-Martin, Marc Gómez-Ventura, Arnau Cordomí, Félix Busqué, Ramon Alibés,* Leonardo Pardo,* and Rafael Franco*

Cite This: *J. Med. Chem.* 2021, 64, 9354−9364

Read Online

ACCESS | Metrics & More | Article Recommendations | Supporting Information

**ABSTRACT:** Cannabidiol (CBD), the second most abundant of the active compounds found in the *Cannabis sativa* plant, is of increasing interest because it is approved for human use and is neither euphorizing nor addictive. Here, we design and synthesize novel compounds taking into account that CBD is both a partial agonist, when it binds to the orthosteric site, and a negative allosteric modulator, when it binds to the allosteric site of the cannabinoid $CB_2$ receptor. Molecular dynamic simulations and site-directed mutagenesis studies have identified the allosteric site near the receptor entrance. This knowledge has permitted to perform structure-guided design of negative and positive allosteric modulators of the $CB_2$ receptor with potential therapeutic utility.

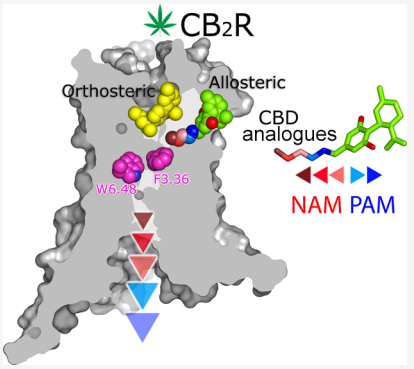


## INTRODUCTION

Cannabidiol (CBD) is the second most abundant of the active compounds found in the *Cannabis sativa* plant (more commonly known as marijuana) (Figure 1). However, in contrast to (−)-*trans*-Δ9-tetrahydrocannabinol (THC), the principal psychoactive constituent of *Cannabis*, CBD is noneuphorizing and nonaddictive. In humans, CBD exhibits a favorable safety profile.[1] Although the exact medical implications are currently being investigated, CBD is generating considerable interest due to its beneficial neuroprotective, antiepileptic, anxiolytic, antipsychotic, and anti-inflammatory properties.[2] Sativex, a 1:1 formulation of CBD and THC, is a cannabinoid medicine approved for the treatment of spasticity due to multiple sclerosis.[3] In addition, an oral solution of CBD (Epidiolex) is the first and only US Food and Drug Administration-approved prescription that is used to treat refractory epilepsy due to Lennox−Gastaut or Dravet syndrome.[4,5] Thus, there is a growing pressure to legalize the use of *Cannabis* products for medical purposes.[6] As a consequence, the CBD scaffold is of increasing interest for medicinal chemists due to its potential therapeutic utility.[7]

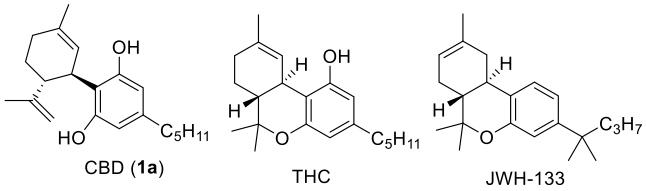


**Figure 1.** Structures of CBD, (−)-*trans*-THC, and JWH-133.

The actions of CBD were first assumed to be mediated through two members of the G-protein-coupled receptor (GPCR) family, the cannabinoid $CB_1$ ($CB_1R$) and $CB_2$ ($CB_2R$) receptors. However, there is evidence that CBD also modulates other molecular targets.[8] These include serotonin, adenosine, opioid, and orphan GPCRs plus non-GPCR proteins.[9] Within the endocannabinoid-related receptors, the pharmacology of CBD shows significant divergences as some authors support high potency as an antagonist of $CB_1R$ and $CB_2R$[10] and others support a very low affinity as a $CB_1R$ agonist.[11] On the other hand, recent results show that CBD may act as a negative allosteric modulator (NAM) of both $CB_1R$[12] and $CB_2R$.[13] In the case of $CB_2R$, CBD would act at micromolar concentration as an agonist[14] and at nanomolar concentration as a NAM.[15]

Here, we have used the recently released structure of $CB_2R$ in its inactive[16] and active,[17,18] $G_i$-bound, conformations to identify the binding mode of CBD in the allosteric binding site

**Received:** March 28, 2021
**Published:** June 23, 2021







https://doi.org/10.1021/acs.jmedchem.1c00561
*J. Med. Chem.* 2021, 64, 9354−9364

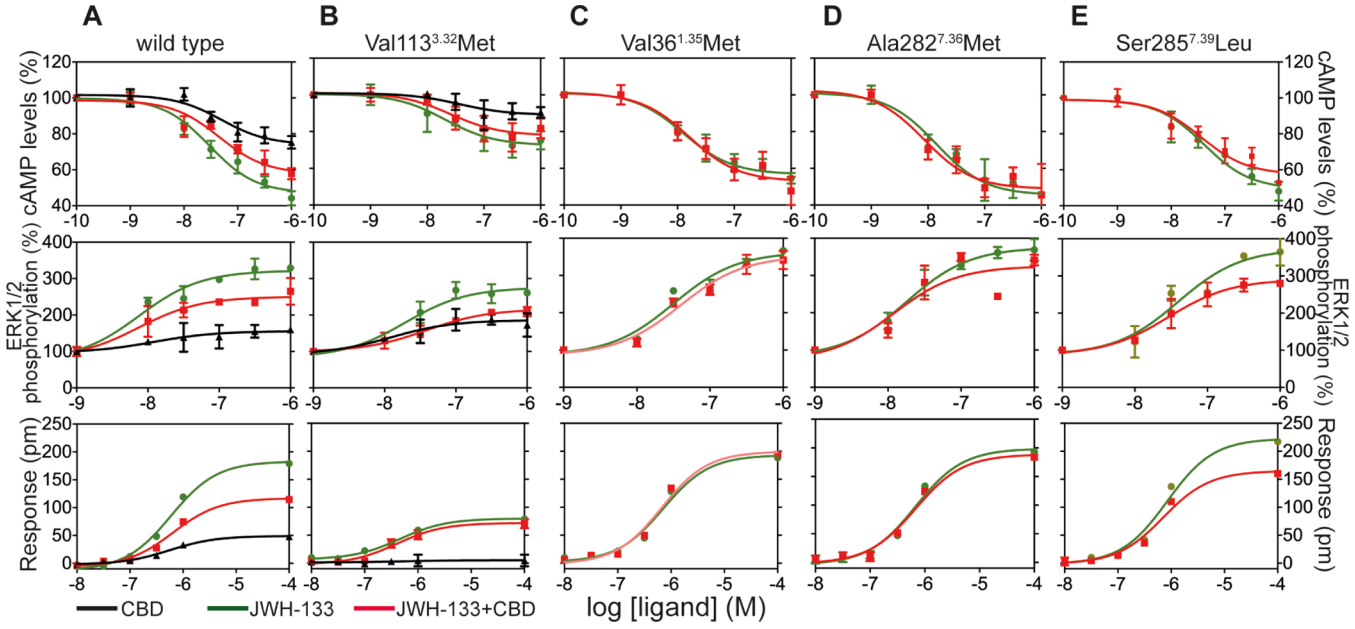


**Figure 2.** Dose−response curves on forskolin-induced cAMP levels (top), on ERK1/2 phosphorylation (middle), and on DMR (bottom), upon the treatment of $CB_2R$-expressing HEK-293T cells [wild-type $CB_2R$ (A) and Val113$^{3.32}$Met (B), Val36$^{1.35}$Met (C), Ala282$^{7.36}$Met (D), or Ser285$^{7.39}$Leu (E) mutants]. Ligands used were CBD (black line), JWH-133 (green), and JWH-133 + CBD (red) ligands. Data for cAMP ($n$ = 9, each in triplicates) are given in percentage (100% represents the forskolin effect), for ERK1/2 phosphorylation ($n$ = 7, each in triplicates) are expressed as percentage with respect to basal levels, and for DMR tracings are representing the picometer (pm) shifts of reflected light wavelengths over time upon ligand treatment.

**Table 1. Functional Properties of JWH-133, CBD, and JWH-133 + CBD at Wild-Type and Mutant $CB_2R$**

| | | cAMP assays | | pERK1/2 assays | | DMR assays | |
|---|---|---|---|---|---|---|---|
| receptor | ligand | $pEC_{50}$ [a] | $E_{max}$ [b] | $pEC_{50}$ [a] | $E_{max}$ [c] | $pEC_{50}$ [a] | $E_{max}$ [d] |
| wild type | CBD | 7.3 ± 0.2 | 74.0 ± 3.0 | 7.9 ± 0.2 | 155.8 ± 4.5 | 6.3 ± 0.1 | 49.1 ± 2.4 |
| | JWH-133 | 7.5 ± 0.1 | 46.0 ± 3.5 | 8.1 ± 0.2 | 322.2 ± 14.6 | 6.2 ± 0.1 | 182.9 ± 8.1 |
| | JWH-133 + CBD | 7.3 ± 0.2 | 57.8 ± 4.1 | 8.1 ± 0.2 | 250.3 ± 8.1 | 6.2 ± 0.1 | 117.0 ± 5.9 |
| V113$^{3.32}$M | CBD | 7.4 ± 0.3 | 89.1 ± 1.9 | 7.9 ± 0.2 | 186.1 ± 7.4 | 6.2 ± 1.1 | 5.3 ± 2.1 |
| | JWH-133 | 7.7 ± 0.1 | 72.5 ± 1.7 | 7.7 ± 0.2 | 275.8 ± 15.3 | 6.3 ± 0.1 | 79.9 ± 3.2 |
| | JWH-133 + CBD | 7.6 ± 0.2 | 77.8 ± 2.2 | 7.4 ± 0.1 | 216.5 ± 5.2 | 6.4 ± 0.2 | 71.9 ± 6.2 |
| V36$^{1.35}$M | JWH-133 | 7.9 ± 0.1 | 56.7 ± 1.7 | 7.5 ± 0.2 | 363.3 ± 25.5 | 6.1 ± 0.1 | 193.2 ± 13.3 |
| | JWH-133 + CBD | 7.8 ± 0.2 | 53.0 ± 3.4 | 7.4 ± 0.2 | 352.7 ± 18.8 | 6.2 ± 0.1 | 199.6 ± 13.8 |
| A282$^{7.36}$M | JWH-133 | 7.9 ± 0.2 | 45.4 ± 4.2 | 7.7 ± 0.1 | 375.7 ± 6.7 | 6.2 ± 0.1 | 198.8 ± 12.3 |
| | JWH-133 + CBD | 8.1 ± 0.2 | 48.8 ± 3.3 | 7.9 ± 0.5 | 325.2 ± 40.9 | 6.2 ± 0.1 | 188.6 ± 10.7 |
| S285$^{7.39}$L | JWH-133 | 7.4 ± 0.2 | 49.3 ± 3.8 | 7.4 ± 0.3 | 373.5 ± 31.5 | 6.1 ± 0.1 | 222.6 ± 14.0 |
| | JWH-133 + CBD | 7.4 ± 0.2 | 57.4 ± 4.7 | 7.5 ± 0.1 | 291.1 ± 8.1 | 6.1 ± 0.1 | 164.9 ± 11.0 |

[a] pEC50 (nM). [b] $E_{max}$ (%), the maximum decrease of forskolin-stimulated cAMP levels (normalized to 100%). [c] $E_{max}$ (%), the maximum increase of ERK1/2 phosphorylation expressed as a percentage of basal (normalized to 100%). [d] $E_{max}$, the maximum increase of picometer shifts of reflected light wavelengths expressed as a value above basal.

by molecular dynamic (MD) simulations and site-directed mutagenesis studies. This knowledge has permitted to perform structure-guided design of NAMs and positive allosteric modulators (PAMs) of $CB_2R$. The designed compounds are relevant because the combination of orthosteric agonists with PAMs could represent a therapeutic approach for neurodegenerative disorders and neuropathic pain.[19] Until now, the only reported allosteric modulators of $CB_2R$, in addition to CBD,[15] are PAMs: the endogenous 12-residue peptide pepcan-12[20] and a synthetic small molecule.[21]

## RESULTS AND DISCUSSION

**CBD Is Both a Partial Agonist and a Negative Allosteric Modulator.** We have first compared the agonist-induced signaling response of CBD with JWH-133, a potent and selective $CB_2R$ agonist, in cAMP production, phosphorylation of signal-regulated kinases (pERK1/2), and label-free dynamic mass redistribution (DMR) assays that enable real-time detection of integrated cellular responses in living cells[22] (Figure 2A and Table 1). These correspond to different steps of the signaling pathways. Cells stimulated with forskolin and treated with JWH-133 or CBD showed reduced cAMP production, as expected for $G_i$-coupled receptors. For the ERK1/2 pathway, both JWH-133 and CBD increased ERK1/2 phosphorylation. Finally, DMR assays also showed an increase of response by JWH-133 and CBD action. Thus, CBD is, relative to JWH-133, a partial agonist in all these assays because the decrease of cAMP or increase of ERK1/2


https://doi.org/10.1021/acs.jmedchem.1c00561
J. Med. Chem. 2021, 64, 9354−9364

phosphorylation or increase of DMR response is of less magnitude. Figure S1 shows proposed computer models of JWH-133 and CBD bound to the orthosteric binding site of $CB_2R$, superimposed to the crystal structure of $CB_2R$ in complex with the structurally similar AM12033 ligand.[18] CBD and JWH-133 are similar in structure, so they both might elicit their agonist action by binding at the orthosteric binding site of $CB_2R$ in a similar manner. In order to validate this hypothesis, we mutated the side chain of Val113$^{3.32}$, which is centrally located in the orthosteric cavity (Figure S1), to the much larger Met side chain (Figure 2B and Table 1). As expected, the Val113$^{3.32}$Met mutation impairs the signaling of both CBD and JWH-133, indicating the binding at the orthosteric site.

Figure 2A and Table 1 also show the effect of CBD on the signaling responses of JWH-133 (JWH-133 + CBD). Clearly, CBD blocks the decrease of forskolin-induced cAMP triggered by JWH-133. Similar effects are observed in the other signaling pathways in which CBD blocks the increase of pERK1/2 and DMR responses. Thus, CBD is, in all these assays, a NAM that decreases the efficacy of the orthosteric JWH-133 agonist.

**CBD Also Binds in an Allosteric Cavity near the Receptor Entrance.** It was proposed that ligands binding a small cavity at the entrance of the orthosteric binding site could act as allosteric modulators,[23] as shown in the crystal structure of the muscarinic M2 receptor simultaneously bound to an orthosteric agonist and a PAM.[24] However, in cannabinoid receptors, and in other GPCRs for lipid mediators, the extracellular N-terminus and ECL2 fold over the ligand-binding pocket blocking the access to the orthosteric binding cavity from the extracellular environment.[25] Previous ligand-binding pathway simulations have shown that binding of lipid-like ligands to a lipid-specific GPCR is through a narrow channel between transmembrane helices (TMs) 1 and 7 that opens toward the lipid bilayer.[26] We have recently used this channel to design bitopic ligands of $CB_2R$.[27] Furthermore, superimposition of the computer model of $CB_2R$ in complex with JWH-133 to the crystal structure of $CB_1R$ in complex with the antagonist AM6538 shows that AM6538 occupies, in addition to the orthosteric binding site, a "side pocket"[28] that is adjacent to JWH-133 near TMs 1 and 7 (Figure S2). Thus, we proposed that CBD, acting as a NAM, binds in an allosteric binding site located at the entrance of the receptor near TMs 1 and 7. Multiple binding sites have been described for $CB_1R$.[29]

In order to better delineate this allosteric binding site, we performed unbiased 1 $\mu$s MD simulations of JWH-133 bound to the $CB_2R$–$G_i$ complex (Figure S3). Allosteric binding site exploration, conducted on structure snapshots extracted from this simulation, together with molecular docking of CBD into these identified cavities (Figure S4) has permitted to propose the binding mode of CBD into an allosteric binding site close to TMs 1 and 7 (Figure 3). In this computational model, the propenyl-methylcyclohexene moiety of CBD points toward the entrance channel between TMs 1 and 7 and the pentyl chain points toward the intracellular side. In detail, the propane substituent is located between Val36$^{1.35}$ and Ala282$^{7.36}$. With the aim of experimentally verifying this model, we mutated the side chains of Val36$^{1.35}$ (Figure 2C) and Ala282$^{7.36}$ (Figure 2D) to the much larger Met side chain. As expected, these mutations completely impair the NAM effect of CBD on the JWH-133 agonist (Table 1) by occupying the volume of the proposed allosteric binding site. Moreover, we also mutated Ser285$^{7.39}$ to Leu to verify the potential hydrogen bond

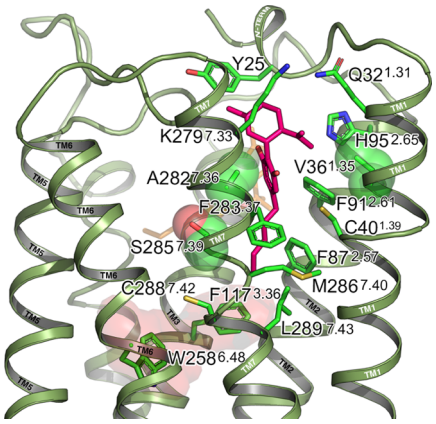


**Figure 3.** Detailed view of the docking model (Figure S4) of CBD (magenta sticks) into an allosteric binding site and JWH-133 (transparent orange sticks) into the orthosteric binding site of $CB_2R$ (green ribbons). The stability of this model was evaluated by MD simulation (Figure S5). The Val36$^{1.35}$, Ala282$^{7.36}$, and Ser285$^{7.39}$ residues mutated to verify the proposed binding mode of CBD are shown in green spheres. Phe117$^{3.36}$ and Trp258$^{6.48}$, which have been described as conformational toggle or trigger switches involved in the initial agonist-induced receptor activation, are highlighted with red transparent surfaces.

between Ser and one of the hydroxyl substituents of the *meta*-benzenediol moiety. This mutation only partly impairs the NAM effect of CBD (Figure 2E and Table 1).

The pentyl chain of CBD expands toward an intracellular hydrophobic cavity formed by Phe87$^{2.57}$, Cys288$^{7.42}$, Leu289$^{7.43}$, and, importantly, Phe117$^{3.36}$ (Figure 3). Phe$^{3.36}$ and Trp$^{6.48}$ have been described as conformational toggle or trigger switches involved in the initial agonist-induced receptor activation in $CB_1R$[34,35] and other GPCRs.[36−39] Thus, the pentyl chain of CBD in its allosteric binding mode might modulate receptor activation.

**Chain Length Determines the NAM or PAM Character of the Allosteric Modulator.** Our simulations suggest that the ability of CBD to block the active state of $CB_2R$ (NAM activity) is due to the insertion of the pentyl chain inside the hydrophobic pocket between TMs 2, 3, and 7. We have tested this hypothesis by measuring the activation of $CB_2R$ using CBD analogues of different chain lengths. We have synthesized CBD (**1a**) and CBD analogues **1b−e** with decreasing ($n$ = 1, 2, and 3) and increasing ($n$ = 5) numbers of methylene units in the hydrophobic chain with respect to CBD ($n$ = 4) while keeping the rest of the molecule identical (Scheme 1).

CBD and analogues have been synthesized by several methods, among which the Lewis acid-catalyzed Friedel−Crafts reaction of cyclic allylic alcohols with resorcinol derivatives has given satisfactory results.[40] However, the main drawback of this arylation reaction is the formation of side regioisomers, coming from the attack of the resorcinol at the 4/6 positions that decrease the yield and make the product isolation difficult.[41] Here, we have followed a practical approach that avoids the formation of the side regioisomers by using protected 4,6-dihalo resorcinols in the coupling reaction.[41] The compounds were prepared as depicted in Scheme 1.

The functional properties of compounds **1a−1e** were evaluated through cAMP assays using HEK293 cells stably expressing $CB_2R$ and treating with forskolin to activate adenyl cyclase (Figure 4 and Table 2). Remarkably, the ethyl or


https://doi.org/10.1021/acs.jmedchem.1c00561
J. Med. Chem. 2021, 64, 9354−9364

**Scheme 1. Synthesis of CBD (1a, $n$ = 4) and CBD Analogues 1b−e with Decreasing (1b−1d, $n$ = 1−3) and Increasing (1e, $n$ = 5) Numbers of Methylene Units**[a]

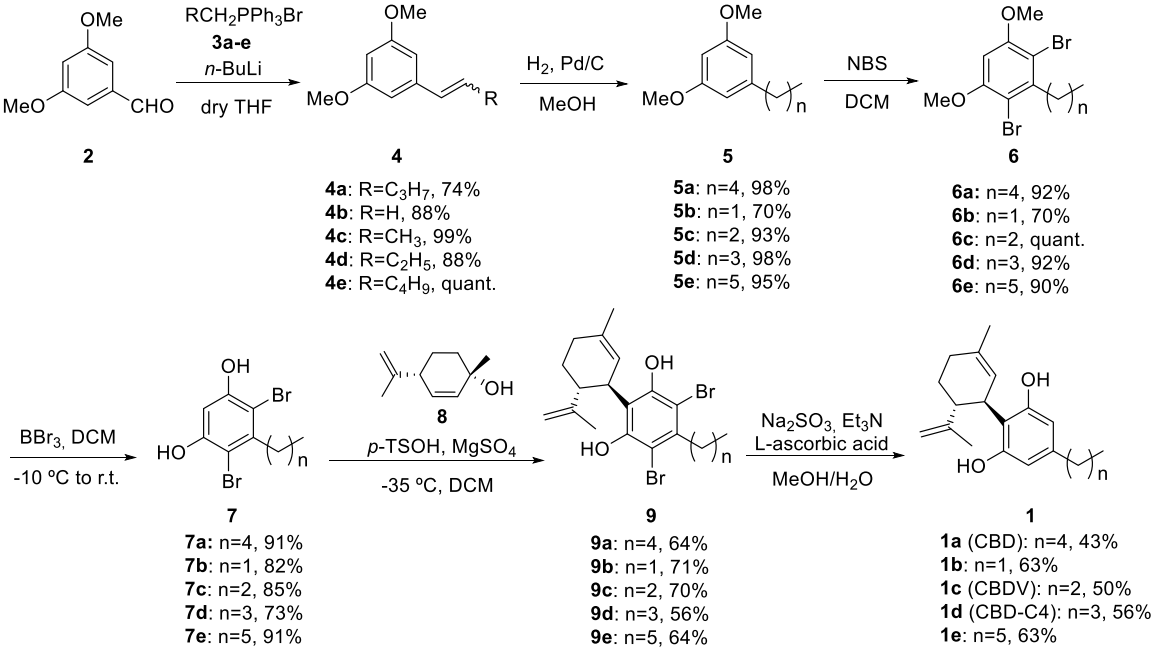


[a]The synthesis began by the Wittig reaction of the ylide of **3a−e** with commercially available 3,5-dimethoxybenzaldehyde, **2**, to deliver olefins **4a−e** as mixtures of *Z* and *E* isomers, which were conveniently reduced with hydrogen under pressure to the C-5 alkyl resorcinol derivatives **5a−e**.[30] Regioselective electrophilic aromatic bromination of **5a−e** using 2.3 equiv of *N*-bromosuccinimide (NBS) in DCM at rt produced exclusively the 4,6-dibrominated products **6a−e** in good yields.[31] Then, the methyl ether-protecting groups were removed with boron tribromide to generate the key resorcinol intermediates **7a−e** which were submitted to the coupling reaction with (1*S*,4*R*)-4-isopropenyl-1-methyl-2-cyclohexen-1-ol, **8**, under a Lewis acid catalyst.[32] For this purpose, different acids were screened (*p*-TsOH, $BF_3{\cdot}OEt_2$, and $AlCl_3$) and among these, *p*-TsOH was found to be the best catalyst. Thus, Friedel−Craft alkylation of resorcinols **7a−e** with **8** under *p*-TsOH catalysis in DCM furnished adducts **9a−e** as single diastereomers. Finally, reductive didehalogenation using sodium sulfite[33] in the presence of $Et_3N$ in a mixture of MeOH and $H_2O$ at 75 °C delivered the targeted cannabinoids **1a−e**. The optical rotation of the prepared CBD was consistent with the literature [[$\alpha$]D22 = −121.4 (*c* 1.00, EtOH)[32] and [$\alpha$]D20 = −122.0 (*c* 1.10, EtOH]. Complete experimental details and analytical data for the synthetized compounds are included in the Experimental Section.

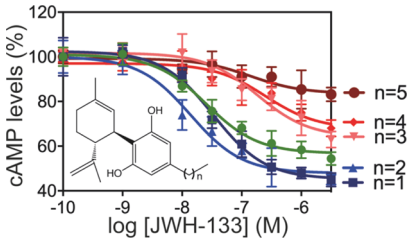


**Figure 4.** Decrease of forskolin-induced cAMP (normalized to 100%), in HEK-293T cells, upon the stimulation of wild-type $CB_2R$ with the orthosteric JWH-133 agonist (green line) and in conjunction with CBD analogues with decreasing (**1b−1d**, $n$ = 1−3) and increasing (**1e**, $n$ = 5) numbers of methylene units in the hydrophobic chain with respect to CBD (**1a**, $n$ = 4). Compounds with chains of $n$ = 1−2 are PAMs (blue lines) and with $n$ = 3−5 are NAMs (red lines).

propyl chains make compounds **1b** and **1c** ($n$ = 1 and 2) PAMs, as they facilitate the decrease of forskolin-induced cAMP triggered by JWH-133 ($E_{max}$ 45.3 or 48.0 vs 56.0). Compound **1c** is more potent than **1b**, as the propyl chain of **1c** left-shifts the dose−response curve (0.4 log units) relative to the ethyl chain of **1b**. The butyl chain makes compound **1d** ($n$ = 3) a NAM, which is very similar in properties to CBD ($n$ = 4). In agreement with our hypothesis, the extension of the number of methylene units makes the hexyl chain of compound **1e** ($n$ = 5) a more efficacious NAM ($E_{max}$ 83.5), relative to CBD ($E_{max}$ 67.8). The influence of ligand chain length in the activation of lipid GPCRs has been described.[42]

**Table 2. Modulation of the Agonist Signal of JWH-133 by Designed Allosteric Modulators 1a−1e**

| orthosteric site | allosteric site | $pEC_{50}$[a] | $E_{max}$[b] | max. effect (% of JWH-133)[c] |
|---|---|---|---|---|
| JWH-133 | none | 7.6 ± 0.1 | 56.0 ± 1.3 | 100% |
| JWH-133 | **1b** ($n$ = 1) | 7.5 ± 0.2 | 45.3 ± 1.5 | 124% PAM |
| JWH-133 | **1c** ($n$ = 2) | 7.9 ± 0.2 | 48.0 ± 1.8 | 118% PAM |
| JWH-133 | **1d** ($n$ = 3) | 6.7 ± 0.2 | 64.1 ± 3.2 | 82% NAM |
| JWH-133 | **1a** ($n$ = 4) | 6.6 ± 0.2 | 67.8 ± 3.3 | 73% NAM |
| JWH-133 | **1e** ($n$ = 5) | 6.9 ± 0.2 | 83.5 ± 2.3 | 38% NAM |

[a]$pEC_{50}$ (nM). [b]$E_{max}$ (%), the maximum inhibition of forskolin-stimulated cAMP levels (normalized to 100%). These values were calculated using nonlinear regression analysis. Data are expressed as the mean ± SEM of at least three independent experiments performed in triplicates. [c]The efficiency (in %) of **1a−1e** together with JWH-133 in decreasing cAMP relative to JWH-133 (100%).

PAM **1c** ($n$ = 2) and NAM **1e** ($n$ = 5) were modeled in the $CB_2R{-}G_i$ complex and performed unbiased MD simulations to explore the influence of the chain length in the conformational toggle or trigger switches (Figure 5). The shorter chain of


https://doi.org/10.1021/acs.jmedchem.1c00561
J. Med. Chem. 2021, 64, 9354−9364

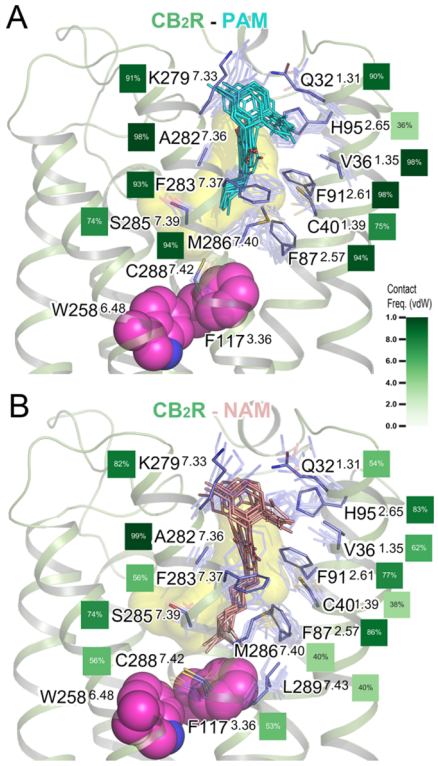


**Figure 5.** (A,B) MD simulation snapshots (10 structures collected every 100 ns) of $CB_2R$–$G_i$ (only the initial structure is shown for clarity) in complex with the JWH-133 agonist (yellow surface) bound to the orthosteric site and PAM **1c** [cyan sticks, (A)] or NAM **1e** [salmon sticks, (B)] bound to the allosteric site. Conformational toggle/trigger switches are shown in pink spheres ($Phe117^{3.36}$ and $W258^{6.48}$). Calculated frequency contacts (%) between side-chain residues of $CB_2R$ (blue sticks) involved in stable interactions with PAM **1c** or NAM **1e** during MD simulations are displayed in squares, color-coded according to the shown scale. Contact frequency analysis was conducted with the GetContacts software package.[43]

PAM **1c** does not interact with $Phe117^{3.36}$, $Cys288^{7.42}$, or $Leu289^{7.43}$, whereas the longer chain of NAM **1e** does. The interaction of the long hexyl chain of NAM **1e** with $Phe117^{3.36}$ favors its inactive trans conformation, in contrast to the active *gauche+* conformation favored by JWH-133 and PAM **1c** (Figure S6).

## CONCLUSIONS

It has been suggested that cannabinoid ligands could fill the therapeutic gap between opioids and nonsteroidal anti-inflammatories in multiple moderate pain conditions, but these compounds can have significant undesirable side effects. This limitation can be avoided by designing ligands that act on $CB_2R$, instead of $CB_1R$, due to their lack of adverse psychotropic effects[44] and designing PAMs that increase the response of the orthosteric endogenous agonist to limit adverse effects.[19] Accordingly, we have designed and synthesized in this article PAMs of $CB_2R$ using the natural product CBD as a scaffold that might be useful for the treatment of pain without producing tolerance or dependence.[45,46]

## EXPERIMENTAL SECTION

**Synthetic Procedures and Compound Characterization.** Commercially available reagents were used as received. Solvents were dried by distillation over the appropriate drying agents. All reactions were monitored by analytical thin-layer chromatography (TLC) using silica gel 60-precoated aluminum plates (0.20 mm thickness). Flash column chromatography was performed using silica gel Geduran SI 60 (40–63 $\mu$m). $^1$H NMR and $^{13}$C NMR spectra were recorded at 250, 360, and 400 MHz and 90 and 100 MHz, respectively. Proton chemical shifts are reported in parts per million ($\delta$) ($CDCl_3$, $\delta$ 7.26 or $CD_3OD$, $\delta$ 3.31). Carbon chemical shifts are reported in parts per million ($\delta$) ($CDCl_3$, $\delta$ 77.16 or $CD_3OD$, $\delta$ 49.00). NMR signals were assigned with the help of heteronuclear single-quantum coherence. Infrared peaks are reported in $cm^{-1}$. The purity of all final compounds was ≥95% as determined by quantitative one-dimensional (1D) $^1$H NMR (qHNMR) experiments using dimethylsulfone ($DMSO_2$, 99.8% pure) as the internal calibrant. Melting points were determined on a hot stage and are uncorrected. High-resolution mass spectra were recorded using electrospray ionization (ESI). Optical rotations were measured at 20 ± 3 °C.

**(*Z*)- and (*E*)-1,3-Dimethoxy-5-(pent-1-en-1-yl)benzene (4a).** To a suspension of butyltriphenylphosphonium bromide (7.38 g, 18.17 mmol) in anhydrous tetrahydrofuran (THF) (40 mL), *n*-BuLi (2.5 M in THF, 7.4 mL, 18.50 mmol) was added dropwise at 0 °C. After continuous stirring for 20 min, a solution of 3,5-dimethoxybenzaldehyde, **2**, (2.05 g, 12.32 mmol) in dry THF (60 mL) was slowly added dropwise. Then, the reaction mixture was stirred at room temperature (rt) until the complete consumption of the starting material, TLC (hexanes/EtOAc, 9:1). The reaction was quenched by the slow addition of water (50 mL) and extracted with EtOAc (3 × 40 mL). The combined organic layers were dried over anhydrous $Na_2SO_4$, concentrated, and purified by column chromatography (hexanes/EtOAc, 9:1) to give a 1.3:1 mixture of (*Z*)- and (*E*)-olefins **4a** (1.88 g, 9.11 mmol, 74% yield) as a colorless oil. (*E*)-**4a**[47] $^1$H NMR (360 MHz, $CDCl_3$): $\delta$ 6.54 (d, $J_{4,2} = J_{6,2}$ = 2.2 Hz, 2H, H-4, H-6), 6.40–6.20 (m, 3H, H-2, H-1′, H-2′), 3.82 (s, 6H, 3-OC$H_3$/5-OC$H_3$), 2.21 (q, $J_{3',2'/4'}$ = 7.2 Hz, 2H, H-3′), 1.55–1.45 (m, 2H, H-4′), and 0.99–0.94 (m, 3H, H-5′); $^{13}$C NMR (90 MHz, $CDCl_3$): $\delta$ 161.0 ($C_1$, $C_3$), 140.1 ($C_5$), 131.7 ($C_{2'}$), 129.9 ($C_{1'}$), 104.1 ($C_4$, $C_6$), 99.2 ($C_2$), 55.4 (2×-OCH$_3$), 35.2 ($C_{3'}$), 22.6 ($C_{4'}$), and 13.9 ($C_{5'}$). (*Z*)-**4a**: $^1$H NMR (360 MHz, $CDCl_3$): $\delta$ 6.47 (d, $J_{4,2} = J_{6,2}$ = 2.2 Hz, 2H, H-4, H-6), 6.40–6.35 (m, 2H, H-2, H-1′), 5.69 (dt, $J_{2',1'}$ = 11.7 Hz, $J_{2',3'}$ = 7.2 Hz, 1H, H-2′), 2.34 (q, $J_{3',2'/4'}$ = 7.3 Hz, 2H, H-3′), 1.50 (q, $J_{4',2'/3'}$ = 7.3 Hz, 2H, H-4′), and 0.96 (q, $J_{5',4'}$ = 7.3 Hz, 2H, H-5′); $^{13}$C NMR (90 MHz, $CDCl_3$): $\delta$ 160.6 ($C_1$, $C_3$), 139.8 ($C_5$), 133.7 ($C_{2'}$), 128.9 ($C_{1'}$), 107.0 ($C_4$, $C_6$), 98.8 ($C_2$), 55.4 (2×-OCH$_3$), 30.9 ($C_{3'}$), 23.3 ($C_{4'}$), and 14.0 ($C_{5'}$).

**1,3-Dimethoxy-5-vinylbenzene (4b).** The synthesis of **4b**[48] was performed as described for **4a** by using methyltriphenylphosphonium bromide (6.51 g, 18.20 mmol) in dry THF (35 mL), *n*-BuLi (2.5 M in THF, 7.4 mL, 18.38 mmol), and **2** (2.01 g, 12.08 mmol) in dry THF (60 mL). Yield **4b**: 88% (1.74 g, 10.61 mmol) as a colorless oil: $^1$H NMR (360 MHz, $CHCl_3$): $\delta$ 6.66 (dd, $J_{trans}$ = 17.5 Hz, $J_{cis}$ = 10.9 Hz, 1H, H-1′), 6.57 (d, $J_{4,2} = J_{6,2}$ = 2.4 Hz, 2H, H-4, H-6), 6.39 (t, $J_{2,4} = J_{2,6}$ = 2.4 Hz, 1H, H-2), 5.73 (dd, $J_{trans}$ = 17.5 Hz, $J_{gem}$ = 0.9 Hz, 1H, H-2′a), 5.25 (dd, $J_{cis}$ = 10.9 Hz, $J_{gem}$ = 0.9 Hz, 1H, H-2′b), and 3.81 (s, 6H, 1-OC$H_3$/3-OC$H_3$); $^{13}$C NMR (90 MHz, $CDCl_3$): $\delta$ 161.0 ($C_1$, $C_3$), 139.7 ($C_5$), 136.9 ($C_{1'}$), 114.5 ($C_{2'}$), 104.4 ($C_4$, $C_6$), 100.1 ($C_2$), and 55.4 (2×-OCH$_3$).

**(*Z*)- and (*E*)-1,3-Dimethoxy-5-(prop-1-en-1-yl)benzene (4c).** A mixture of olefins (*Z*)- and (*E*)-**4c** was prepared as described for **4a** by using ethyltriphenylphosphonium bromide (6.70 g, 18.53 mmol) in dry THF (30 mL), *n*-BuLi (2.5 M in THF, 7.2 mL, 18.05 mmol), and **2** (2.07 g, 12.47 mmol) in dry THF (60 mL). Yield **4c** (*Z*/*E*, 1:1.2): 99% (2.20 g, 12.34 mmol) as a colorless oil. (*E*)-**4c**:[48] $^1$H NMR (360 MHz, $CD_3OD$): $\delta$ 6.48 (m, 2H, H-4, H-6), 6.37–6.20 (m, 3H, H-2, H-1′, H-2′), 3.76 (s, 6H, 1-OC$H_3$/3-OC$H_3$), and 1.88–1.84 (m, 3H, H-3′); $^{13}$C NMR (90 MHz, $CD_3OD$): $\delta$ 162.4 ($C_1$, $C_3$), 141.3 ($C_5$), 132.4 ($C_{1'}$), 126.4 ($C_{2'}$), 104.9 ($C_4$, $C_6$), 99.9 ($C_2$), 55.6 (2×-OCH$_3$), and 18.5 ($C_{3'}$). (*Z*)-**4c**: $^1$H NMR (360 MHz, $CD_3OD$): $\delta$ 6.42 (m, 2H, H-4, H-6), 6.37–6.20 (m, 2H, H-2, H-1′), 5.75 (m, 1H, H-2′), 3.75 (s, 6H, 1-OC$H_3$/3-OC$H_3$), and 1.88–1.84 (m, 3H, H-3′); $^{13}$C NMR (90 MHz, $CD_3OD$): $\delta$ 162.0 ($C_1$, $C_3$), 140.7 ($C_5$),


https://doi.org/10.1021/acs.jmedchem.1c00561
J. Med. Chem. 2021, 64, 9354–9364

131.1 ($C_{1'}$), 127.7 ($C_{2'}$), 107.9 ($C_4$, $C_6$), 99.6 ($C_2$), 55.7 (2×-$OCH_3$), and 14.9 ($C_{3'}$).

**(*Z*)- and (*E*)-1-(But-1-en-1-yl)-3,5-dimethoxybenzene (4d).** The synthesis of a mixture of olefins (*Z*)- and (*E*)-**4d** was performed as described for **4a** by using propyltriphenylphosphonium bromide (7.10 g, 18.42 mmol) in dry THF (40 mL), *n*-BuLi (2.5 M in THF, 7.2 mL, 18.05 mmol), and **2** (2.03 g, 12.19 mmol) in dry THF (60 mL). Yield **4d** (*Z*/*E*, 1:1.5): 88% (2.05 g, 10.66 mmol) as a colorless oil: HRMS (ESI$^+$) calcd for $[C_{24}H_{16}O_2 + H]^+$ ($[M + H]^+$), 193.1229; found, 193.1220. IR (ATR): 2960, 1591, 1457, 1204, 1152, 1065, and 826 cm$^{-1}$. (*E*)-**4d**: $^1$H NMR (360 MHz, $CDCl_3$): $\delta$ 6.52 (d, $J_{2,4} = J_{6,4}$ = 2.3 Hz, 2H, H-2, H-6), 6.34 (d, $J_{4,2} = J_{4,2}$ = 2.3 Hz, 1H, H-4), 6.37−6.22 (m, 2H, H-1′, H-2′), 3.80 (s, 6H, 3-OC$H_3$/5-OC$H_3$), 2.22 (m, 2H, H-3′), and 1.12−1.05 (m, 3H, H-4′); $^{13}$C NMR (90 MHz, $CDCl_3$): $\delta$ 161.0 ($C_3$, $C_5$), 140.1 ($C_1$), 133.3 ($C_{1'}$/$C_{2'}$), 128.9 ($C_{1'}$/$C_{2'}$), 104.1 ($C_2$, $C_6$), 99.2 ($C_4$), 55.4 (2×-$OCH_3$), 26.1 ($C_{3'}$), and 13.7 ($C_{4'}$). (*Z*)-**4d**: $^1$H NMR (360 MHz, $CDCl_3$): $\delta$ 6.44 (d, $J_{2,4} = J_{6,4}$ = 2.2 Hz, 2H, H-2, H-6), 6.37−6.22 (m, 2H, H-4, H-1′), 5.65 (m, 1H, H-2′), 3.80 (s, 6H, 3-OC$H_3$/5-OC$H_3$), 2.36 (m, 2H, H-3′), and 1.12−1.05 (m, 3H, H-4′); $^{13}$C NMR (90 MHz, $CDCl_3$): $\delta$ 160.6 ($C_3$, $C_5$), 139.8 ($C_1$), 135.4 ($C_{2'}$), 128.3 ($C_{1'}$), 106.9 ($C_2$, $C_6$), 98.8 ($C_4$), 55.4 (2×-$OCH_3$), 22.3 ($C_{3'}$), and 14.6 ($C_{4'}$).

**(*Z*)- and (*E*)-1-(Hex-1-en-1-yl)-3,5-dimethoxybenzene (4e).** A mixture of olefins (*Z*)- and (*E*)-**4e** was prepared as described for **4a** by using pentyltriphenylphosphonium bromide (6.15 g, 14.89 mmol) in dry THF (25 mL), *n*-BuLi (2.5 M in THF, 6.0 mL, 14.89 mmol), and **2** (1.65 g, 9.93 mmol) in dry THF (85 mL). Yield **4e** (*Z*/*E*, 1.2:1): quant. (2.19 g, 9.93 mmol) as a colorless oil: HRMS (ESI$^+$) calcd for $[C_{14}H_{20}O_2 + H]^+$ ($[M + H]^+$), 221.1542; found, 221.1535. IR (ATR): 2957, 1591, 1458, 1205, 1154, and 1067 cm$^{-1}$. (*E*)-**4e**: $^1$H NMR (360 MHz, $CDCl_3$): $\delta$ 6.52 (m, 2H, H-2, H-6), 6.37−6.19 (m, 3H, H-4, H-1′, H-2′), 3.80 (s, 6H, 3-OC$H_3$/5-OC$H_3$), 2.22 (m, 2H, H-3′), 1.49−1.36 (m, 4H, H-4′, H-5′), and 0.96−0.89 (m, 3H, H-6′); $^{13}$C NMR (90 MHz, $CDCl_3$): $\delta$ 160.6 ($C_3$, $C_5$), 139.8 ($C_1$), 131.9 ($C_{1'}$/$C_{2'}$), 129.7 ($C_{1'}$/$C_{2'}$), 104.0 ($C_2$, $C_6$), 99.2 ($C_4$), 55.4 (2×-$OCH_3$), 32.8 ($C_{3'}$), 31.6 ($C_{4'}$), 22.4 ($C_{5'}$), and 14.1 ($C_{6'}$). (*Z*)-**4e**: $^1$H NMR (360 MHz, $CDCl_3$): $\delta$ 6.46 (m, 2H, H-2, H-6), 6.37−6.19 (m, 2H, H-2, H-1′), 5.67 (m, 1H, H-2′), 3.80 (s, 6H, 3-OC$H_3$/5-OC$H_3$), 2.36 (m, 2H, H-3′), 1.49−1.36 (m, 4H, H-4′, H-5′), and 0.96−0.89 (m, 3H, H-6′); $^{13}$C NMR (90 MHz, $CDCl_3$): $\delta$ 160.9 ($C_3$, $C_5$), 140.1 ($C_1$), 133.8 ($C_{1'}$/$C_{2'}$), 128.8 ($C_{1'}$/$C_{2'}$), 106.9 ($C_2$, $C_6$), 98.7 ($C_4$), 55.4 (2×-$OCH_3$), 32.3 ($C_{3'}$), 28.6 ($C_{4'}$), 22.6 ($C_{5'}$), and 14.1 ($C_{6'}$).

**1,3-Dimethoxy-5-pentylbenzene (5a).** A stirred solution of **4a** (82 mg, 398 $\mu$mol) and two drops of acetic acid in MeOH (3 mL) were hydrogenated over Pd/C (10% in wt of Pd, 11 mg, 10 $\mu$mol) under 1 atm of $H_2$ for 24 h. Then, the catalyst was removed by filtration over Celite and the solvent was evaporated under reduced pressure to deliver compound **5a**[49] (82 mg, 389 $\mu$mol, 98% yield) as a yellow oil: $^1$H NMR (360 MHz, $CDCl_3$): $\delta$ 6.37 (m, 2H, H-4, H-6), 6.37 (m, 1H, H-2), 3.80 (s, 6H, 1-OC$H_3$/3-OC$H_3$), 2.56 (t, $J_{1',2'}$ = 7.6 Hz, 2H, H-1′), 1.62 (quint, $J_{2',1'/3'}$ = 7.6 Hz, 2H, H-2′), 1.38−1.28 (m, 4H, H-3′, H-4′), and 0.91 (m, 3H, H-5′); $^{13}$C NMR (90 MHz, $CDCl_3$): $\delta$ 160.7 ($C_1$, $C_3$), 145.5 ($C_5$), 105.4 ($C_4$, $C_6$), 97.6 ($C_2$), 55.3 (3-OC$H_3$/5-OC$H_3$), 36.4 ($C_{1'}$), 31.7 ($C_{3'}$), 31.1 ($C_{2'}$), 22.7 ($C_{4'}$), and 14.2 ($C_{5'}$).

**1,3-Dimethoxy-5-ethylbenzene (5b).** Compound **5b**[49] was prepared as described for **5a** by using a solution of **4b** (1.67 g, 10.19 mmol) and two drops of acetic acid in MeOH (60 mL) and Pd/C (10% in wt of Pd, 168 mg, 160 $\mu$mol). Yield **5b**: 70% (1.17 g, 7.01 mmol) as a brown oil: $^1$H NMR (360 MHz, $CDCl_3$): $\delta$ 6.38 (d, $J_{4,2} = J_{6,2}$ = 2.1 Hz, 2H, H-4, H-6), 6.31 (t, $J_{2,4} = J_{2,6}$ = 2.1 Hz 1H, H-2), 3.79 (s, 6H, 1-OC$H_3$/3-OC$H_3$), 2.60 (q, $J_{1',2'}$ = 7.6 Hz, 2H, H-1′), and 1.23 (t, $J_{2',1'}$ = 7.6 Hz, 3H, H-2′); $^{13}$C NMR (90 MHz, $CDCl_3$): $\delta$ 160.9 ($C_1$, $C_5$), 146.9 ($C_5$), 106.0 ($C_4$, $C_6$), 97.6 ($C_2$), 55.4 (2×-$OCH_3$), 29.3 ($C_{1'}$), and 15.6 ($C_{2'}$).

**1,3-Dimethoxy-5-propylbenzene (5c).** Compound **5c**[49] was prepared as described for **5a** by using a solution of **4c** (2.03 g, 11.38 mmol) and two drops of acetic acid in MeOH (70 mL) and Pd/C (10% in wt of Pd, 215 mg, 200 $\mu$mol). Yield **5c**: 93% (1.91 g, 10.60 mmol) as a pale yellow oil: $^1$H NMR (360 MHz, $CDCl_3$): $\delta$ 6.36 (d, $J_{4,2} = J_{6,2}$ = 2.2 Hz, 2H, H-4, H-6), 6.31 (m, 1H, H-2), 3.79 (s, 6H, 1-OC$H_3$/3-OC$H_3$), 2.54 (t, $J_{1',2'}$ = 7.5 Hz, 2H, H-1′), 1.64 (quint, $J_{2',1'/3'}$ = 7.5 Hz, 2H, H-2′), and0.95 (t, $J_{3',2'}$ = 7.5 Hz, 3H, H-3′); $^{13}$C NMR (90 MHz, $CDCl_3$): $\delta$ 160.7 ($C_1$, $C_3$), 145.3 ($C_5$), 106.9 ($C_4$, $C_6$), 97.7 ($C_2$), 55.3 (2×-$OCH_3$), 38.5 ($C_{1'}$), 24.5 ($C_{2'}$), and 14.0 ($C_{3'}$).

**5-Butyl-1,3-dimethoxybenzene (5d).** Compound **5d**[49] was prepared as described for **5a** by using a solution of **4d** (2.05 g, 10.66 mmol) and two drops of acetic acid in MeOH (60 mL) and Pd/C (10% in wt of Pd, 212 mg, 200 $\mu$mol). Yield **5d**: 98% (2.03 g, 10.44 mmol) as a yellow oil: $^1$H NMR (360 MHz, $CDCl_3$): $\delta$ 6.35 (m, 2H, H-4, H-6), 6.30 (m, 1H, H-2), 3.78 (s, 6H, 1-OC$H_3$/3-OC$H_3$), 2.56 (t, $J_{1',2'}$ = 7.6 Hz, 2H, H-1′), 1.59 (quint, $J_{2',1'/3'}$ = 7.6 Hz, 2H, H-2′), 1.36 (sext, $J_{3',2'/4'}$ = 7.5 Hz, 2H, H-3′), and 0.93 (t, $J_{4',3'}$ = 7.4 Hz, 3H, H-4′); $^{13}$C NMR (90 MHz, $CDCl_3$): $\delta$ 160.8 ($C_1$, $C_3$), 145.5 ($C_5$), 106.6 ($C_4$, $C_6$), 97.6 ($C_2$), 55.3 (2×-$OCH_3$), 36.1 ($C_{1'}$), 33.6 ($C_{2'}$), 22.5 ($C_{3'}$), and 14.1 ($C_{4'}$).

**5-Hexyl-1,3-dimethoxybenzene (5e).** Compound **5e** was prepared as described for **5a** by using a solution of **4e** (2.00 g, 9.08 mmol) and two drops of acetic acid in MeOH (70 mL) and Pd/C (10% in wt of Pd, 200 mg, 187 $\mu$mol). Yield **5e**: 95% (1.97 g, 9.07 mmol) as a yellow oil: $^1$H NMR (360 MHz, $CDCl_3$): $\delta$ 6.35 (m, 2H, H-4, H-6), 6.30 (s, 1H, H-2), 3.78 (s, 6H, 1-OC$H_3$/3-OC$H_3$), 2.54 (t, $J_{1',2'}$ = 7.8 Hz, 2H, H-1′), 1.61 (m, 2H, H-2′), 1.33 (m, 6H, H-3′, H-4′, H-5′), and 0.88 (m, 3H, H-6′); $^{13}$C NMR (90 MHz, $CDCl_3$): $\delta$ 160.8 ($C_1$, $C_3$), 145.6 ($C_5$), 106.6 ($C_4$, $C_6$), 97.6 ($C_5$), 55.4 (2×-$OCH_3$), 36.5 ($C_{1'}$), 31.9 ($C_{4'}$), 31.4 ($C_{2'}$), 29.2 ($C_{3'}$), 22.8 ($C_{5'}$), and 14.3 ($C_{6'}$); IR (ATR): 2930, 2856, 1598, 1464, 1210, and 1153 cm$^{-1}$. HRMS (ESI$^+$) calcd for $[C_{14}H_{22}O_2 + H]^+$ ($[M + H]^+$), 223.1698; found, 223.1693.

**2,4-Dibromo-1,5-dimethoxy-3-pentylbenzene (6a).** To a solution of **5a** (515 mg, 2.47 mmol) in $CH_2Cl_2$ (10 mL), NBS (525 mg, 2.95 mmol) was added, and the reaction mixture was stirred at rt for 1 h. Then, another portion of NBS (499 mg, 2.81 mmol) and $CH_2Cl_2$ (5 mL) was added and the mixture was stirred for 1 h. After this time, a third portion of NBS (276 mg, 1.55 mmol) and $CH_2Cl_2$ (3 mL) was added and the mixture was stirred overnight. The reaction was quenched by the slow addition of water (5 mL), and the organic layer was washed with water (5 × 15 mL), dried over anhydrous $Na_2SO_4$, and concentrated under vacuum. The resulting solid was purified by flash column chromatography (hexanes/EtOAc, 9:1) to furnish **6a** as a white solid (806 mg, 2.20 mmol, 92% yield): mp 70−71 °C (from $CH_2Cl_2$); $^1$H NMR (360 MHz, $CDCl_3$): $\delta$ 6.40 (s, 1H, H-6), 3.90 (s, 6H, 1-OC$H_3$/5-OC$H_3$), 3.03 (m, 2H, H-1′), 1.55 (m, 2H, H-2′), 1.39 (m, 4H, H-3′, H-4′), and 0.92 (m, 3H, H-5′); $^{13}$C NMR (90 MHz, $CDCl_3$): $\delta$ 155.9 ($C_1$, $C_5$), 143.5 ($C_3$), 105.4 ($C_2$, $C_4$), 94.9 ($C_6$), 56.7 (2×-$OCH_3$), 37.3 ($C_{1'}$), 32.0 ($C_{2'}$), 27.8 ($C_{3'}$), 22.5 ($C_{4'}$), and 14.2 ($C_{5'}$); IR (ATR): 2928, 1571, 1449, 1423, 1332, 1212, and 1085 cm$^{-1}$. HRMS (ESI$^+$) calcd for $[C_{13}H_{18}Br_2O_2 + Na]^+$ ($[M + Na]^+$), 386.9571; found, 386.9563.

**2,4-Dibromo-3-ethyl-1,5-dimethoxybenzene (6b).** Compound **6b** was prepared as described for **6a** by using a solution of **5b** (1.66 g, 7.02 mmol) in $CH_2Cl_2$ (20 mL; 10 mL; and 5 mL) and NBS (1.29 g, 7.22 mmol; 1.50 g, 8.45 mmol; and 0.79 g, 4.43 mmol). Yield **6b**: 70% (1.60 g, 4.98 mmol) as a pale yellow solid: mp 89−91 °C (from $CH_2Cl_2$); $^1$H NMR (360 MHz, $CDCl_3$): $\delta$ 6.40 (s, 1H, H-6), 3.89 (s, 6H, 1-OC$H_3$/5-OC$H_3$), 3.08 (q, $J_{1',2'}$ = 7.6 Hz, 2H, H-1′), and 1.03 (t, $J_{2',1'}$ = 7.5 Hz, 3H, H-2′); $^{13}$C NMR (90 MHz, $CDCl_3$): $\delta$ 155.9 ($C_1$, $C_5$), 144.3 ($C_3$), 105.1 ($C_2$, $C_4$), 94.9 ($C_6$), 56.6 (2×-$OCH_3$), 30.9 ($C_{1'}$), and 12.5 ($C_{2'}$). IR (ATR): 2943, 1422, 1334, 1092, 1054, and 986 cm$^{-1}$.

**2,4-Dibromo-1,5-dimethoxy-3-propylbenzene (6c).** Compound **6c** was prepared as described for **6a** by using a solution of **5c** (1.91 g, 10.61 mmol) in $CH_2Cl_2$ (40 mL; 20 mL; and 10 mL) and NBS (1.91 g, 10.71 mmol; 1.90 g, 10.69 mmol; and 950 mg, 5.34 mmol). Yield **6c**: quant. (3.58 g, 10.61 mmol) as a white solid: mp 82−84 °C (from $CH_2Cl_2$); $^1$H NMR (360 MHz, $CDCl_3$): $\delta$ 6.40 (s, 1H, H-6), 3.90 (s, 6H, 1-OC$H_3$/5-OC$H_3$), 3.01 (m, 2H, H-1′), 1.58 (m, 2H, H-2′), and 1.03 (t, $J_{3',2'}$ = 7.3 Hz, 3H, H-3′); $^{13}$C NMR (90 MHz, $CDCl_3$): $\delta$ 155.9 ($C_1$, $C_5$), 143.2 ($C_3$), 105.4 ($C_2$, $C_4$), 94.9


https://doi.org/10.1021/acs.jmedchem.1c00561
J. Med. Chem. 2021, 64, 9354−9364

($C_6$), 56.6 (2×-$OCH_3$), 39.2 ($C_{1'}$), 21.6 ($C_{2'}$), and 14.3 ($C_{3'}$); IR (ATR): 2965, 1570, 1447, 1422, 1329, 1209, and 1081 $cm^{-1}$. HRMS ($ESI^+$) calcd for $[C_{11}H_{14}Br_2O_2 + H]^+$ ($[M + H]^+$), 336.9439; found, 336.943.

**2,4-Dibromo-3-butyl-1,5-dimethoxybenzene (6d).** Compound **6d** was prepared as described for **6a** by using a solution of **5d** (2.03 g, 10.44 mmol) in $CH_2Cl_2$ (45 mL; 20 mL; and 10 mL) and NBS (1.94 g, 10.90 mmol; 1.98 g, 11.12 mmol; and 963 mg, 5.41 mmol). Yield **6d**: 92% (3.39 g, 9.64 mmol) as a pale brown solid: mp 64−66 °C (from $CH_2Cl_2$); $^1H$ NMR (360 MHz, $CDCl_3$): $\delta$ 6.40 (s, 1H, H-6), 3.90 (s, 6H, 1-$OCH_3$/5-$OCH_3$), 3.03 (m, 2H, H-1′), 1.50 (m, 2H, H-2′, H-3′), and 0.97 (t, $J_{4',3'}$ = 7.0 Hz, 3H, H-4′); $^{13}C$ NMR (90 MHz, $CDCl_3$): $\delta$ 155.9 ($C_1$, $C_5$), 143.4 ($C_3$), 105.4 ($C_2$, $C_4$), 94.8 ($C_6$), 55.6 (2×-$OCH_3$), 37.1 ($C_{1'}$), 30.3 ($C_{2'}$), 23.0 ($C_{3'}$), and 14.0 ($C_{4'}$); IR (ATR): 2960, 1571, 1449, 1423, 1335, 1211, 1082, and 1052 $cm^{-1}$.

**2,4-Dibromo-3-hexyl-1,5-dimethoxybenzene (6e).** Compound **6e** was prepared as described for **6a** by using a solution of **5e** (1.94 g, 8.72 mmol) in $CH_2Cl_2$ (40 mL; 20 mL; and 10 mL) and NBS (1.86 g, 10.47 mmol; 1.86 g, 10.47 mmol; and 1.0 g, 5.62 mmol). Yield **6e**: 91% (3.01 g, 7.91 mmol) as a pale orange solid: mp 63−65 °C (from $CH_2Cl_2$); $^1H$ NMR (360 MHz, $CDCl_3$): $\delta$ 6.41 (s, 1H, H-6), 3.91 (s, 6H, 1-$OCH_3$/5-$OCH_3$), 3.04 (m, 2H, H-1′), 1.55 (m, 2H, H-2′), 1.45 (m, 2H, H-3′), 1.36 (m, 4H, H-4′, H-5′), and 0.91 (m, 3H, H-6′); $^{13}C$ NMR (90 MHz, $CDCl_3$): $\delta$ 155.9 ($C_1$, $C_5$), 143.4 ($C_3$), 105.4 ($C_2$, $C_4$), 94.8 ($C_6$), 55.6 (2×-$OCH_3$), 37.4 ($C_{1'}$), 31.6 ($C_{4'}$), 29.5 ($C_{3'}$), 28.1 ($C_{2'}$), 22.8 ($C_{5'}$), and 14.3 ($C_{6'}$); IR (ATR): 2928, 2857, 1569, 1450, 1422, 1343, 1209, and 1088 $cm^{-1}$. HRMS ($ESI^+$) calcd for $[C_{14}H_{20}Br_2O_2 + H]^+$ ($[M + H]^+$), 378.9908; found, 378.9905.

**4,6-Dibromo-5-pentylbenzene-1,3-diol (7a).** A solution of $BBr_3$ (1 M in $CH_2Cl_2$, 2.5 mL, 2.5 mmol) was slowly added to a solution of compound **6a** (230 mg, 628 $\mu$mol) in $CH_2Cl_2$ (12 mL) at −10 °C. The reaction mixture was stirred at rt overnight. The reaction was quenched by the slow addition of water (16 mL), and the organic layer was separated. The aqueous layer was extracted with $CH_2Cl_2$ (3 × 8 mL), and the combined organic layer was dried over $Na_2SO_4$, filtered, and concentrated under vacuum. The resulting crude solid product was purified by flash column chromatography (hexanes/EtOAc, 2:1) to furnish **7a** (193 mg, 570 $\mu$mol, 91% yield) as a gray solid: mp 65−66 °C (from $CH_2Cl_2$); $^1H$ NMR (360 MHz, $CDCl_3$): $\delta$ 6.65 (s, 1H, H-2), 5.72 (s, 2H, OH-1/OH-3), 2.92 (m, 2H, H-1′), 1.55 (m, 2H, H-2′), 1.40 (m, 4H, H-3′, H-4′), and 0.93 (m, 3H, H-5′); $^{13}C$ NMR (90 MHz, $CDCl_3$): $\delta$ 152.6 ($C_1$, $C_3$), 141.5 ($C_5$), 104.2 ($C_4$, $C_6$), 100.9 ($C_2$), 37.2 ($C_{1'}$), 31.9 ($C_{2'}$), 27.9 ($C_{3'}$), 22.9 ($C_{4'}$), and 14.2 ($C_{5'}$); IR (ATR): 3427, 3217, 2927, 1577, 1426, 1230, and 1164 $cm^{-1}$. HRMS ($ESI^-$) calcd for $[C_{11}H_{14}Br_2O_2 - H]^-$ ($[M - H]^-$), 334.9282; found, 334.9291.

**4,6-Dibromo-5-ethylbenzene-1,3-diol (7b).** Compound **7b** was prepared as described for **7a** by using a solution of **6b** (1.40 g, 4.32 mmol) in $CH_2Cl_2$ (70 mL) and $BBr_3$ (1 M in $CH_2Cl_2$, 17.2 mL, 24.69 mmol). Yield **7b**: 82% (1.05 g, 3.53 mmol) as a gray solid: mp 105−107 °C (from $CH_2Cl_2$); $^1H$ NMR (360 MHz, $CDCl_3$): $\delta$ 6.66 (s, 1H, H-2), 5.68 (s, 2H, OH-1/OH-3), 2.99 (q, $J_{1',2'}$ = 7.4 Hz, 2H, H-1′), and 1.16 (t, $J_{2',1'}$ = 7.4 Hz, 3H, H-2′); $^{13}C$ NMR (90 MHz, $CDCl_3$): $\delta$ 152.7 ($C_1$, $C_3$), 142.5 ($C_5$), 103.9 ($C_4$, $C_6$), 100.9 ($C_2$), 31.3 ($C_{1'}$), and 12.5 ($C_{2'}$); IR (ATR): 3476, 3240, 1583, 1429, 1336, 1231, and 1165 $cm^{-1}$. HRMS ($ESI^-$) calcd for $[C_8H_8Br_2O_2 - H]^-$ ($[M - H]^-$), 292.8813; found, 292.8821.

**4,6-Dibromo-5-propylbenzene-1,3-diol (7c).** Compound **7c**[41] was prepared as described for **7a** by using a solution of **6c** (2.04 g, 6.89 mmol) in $CH_2Cl_2$ (80 mL) and $BBr_3$ (1 M in $CH_2Cl_2$, 24.0 mL, 24.00 mmol). Yield **7c**: 85% (1.82 g, 5.87 mmol) as a gray solid: mp 89−91 °C (from $CH_2Cl_2$); $^1H$ NMR (360 MHz, $CDCl_3$): $\delta$ 6.66 (s, 1H, H-2), 5.65 (s, 2H, OH-1/OH-3), 2.91 (m, 2H, H-1′), 1.59 (t, $J_{2',1'/3'}$ = 7.5 Hz, 2H, H-2′), and 1.04 (t, $J_{3',2'}$ = 7.4 Hz, 3H, H-3′); $^{13}C$ NMR (90 MHz, $CDCl_3$): $\delta$ 152.7 ($C_1$, $C_3$), 141.3 ($C_5$), 104.3 ($C_4$, $C_6$), 100.9 ($C_2$), 39.6 ($C_{1'}$), 21.7 ($C_{2'}$), and 14.2 ($C_{3'}$); IR (ATR): 3422, 3155, 2968, 1581, 1423, 1339, and 1238 $cm^{-1}$.

**4,6-Dibromo-5-propylbenzene-1,3-diol (7d).** Compound **7d** was prepared as described for **7a** by using a solution of **6d** (2.00 g, 5.68 mmol) in $CH_2Cl_2$ (80 mL) and $BBr_3$ (1 M in $CH_2Cl_2$, 22.7 mL, 22.7 mmol). Yield **7d**: 73% (1.34 g, 4.13 mmol) as a gray solid: mp 96−97 °C (from $CH_2Cl_2$); $^1H$ NMR (360 MHz, $CDCl_3$): $\delta$ 6.65 (s, 1H, H-2), 5.65 (s, 2H, OH-1/OH-3), 2.94 (m, 2H, H-1′), 1.49 (m, 4H, H-2′, H-3′), and 0.98 (t, $J_{4',3'}$ = 7.1 Hz, 3H, H-4′); $^{13}C$ NMR (90 MHz, $CDCl_3$): $\delta$ 152.7 ($C_1$, $C_3$), 141.5 ($C_5$), 104.2 ($C_4$, $C_6$), 100.8 ($C_2$), 37.5 ($C_{1'}$), 30.3 ($C_{2'}$), 22.9 ($C_{3'}$), and 14.0 ($C_{4'}$); IR (ATR): 3432, 3224, 2962, 1582, 1424, 1260, and 1145 $cm^{-1}$. HRMS ($ESI^-$) calcd for $[C_{10}H_{12}Br_2O_2 - H]^-$ ($[M - H]^-$), 320.9126; found, 320.9138.

**4,6-Dibromo-5-hexylbenzene-1,3-diol (7e).** Compound **7e** was prepared as described for **7a** by using a solution of **6e** (1.00 g, 2.63 mmol) in $CH_2Cl_2$ (50 mL) and $BBr_3$ (1 M in $CH_2Cl_2$, 10.5 mL, 10.50 mmol).Yield **7e**: 91% (846 mg 2.40 mmol) as a gray solid: mp 55−53 °C (from $CH_2Cl_2$); $^1H$ NMR (360 MHz, $CDCl_3$): $\delta$ 6.65 (s, 1H, H-2), 5.67 (s, 2H, OH-1/OH-3), 2.92 (m, 2H, H-1′), 1.52 (m, 2H, H-2′), 1.43 (m, 2H, H-3′), 1.33 (m, 4H, H-4′, H-5′), and 0.90 (m, 3H, H-6′); $^{13}C$ NMR (90 MHz, $CDCl_3$): $\delta$ 152.6 ($C_1$, $C_3$), 141.6 ($C_5$), 104.2 ($C_4$, $C_6$), 100.8 ($C_2$), 37.8 ($C_{1'}$), 31.6 ($C_{4'}$), 29.4 ($C_{3'}$), 28.1 ($C_{2'}$), 22.9 ($C_{5'}$), and 14.2 ($C_{6'}$); IR (ATR): 3427, 3173, 2926, 1578, 1421, 1341, and 1231 $cm^{-1}$. HRMS ($ESI^-$) calcd for $[C_{12}H_{16}Br_2O_2 - H]^-$ ($[M - H]^-$), 348.9439; found, 348.9449.

**4,6-Dibromo-2-[(1*R*,6*R*)-6-isopropenyl-3-methylcyclohex-2-en-1-yl]-5-pentylbenzene-1,3-diol (9a).** A mixture of **7a** (152 mg, 450 $\mu$mol), (1*S*,4*R*)-1-methyl-4-(prop-1-en-2-yl)cyclohex-2-en-1-ol, **8** (82 mg, 540 $\mu$mol), and magnesium sulfate (136 mg, 1.16 mmol) in dry $CH_2Cl_2$ (5 mL) was cooled to −35 °C in a $N_2$/Ar atmosphere. Then, *p*-toluenesulfonic acid monohydrate (43 mg, 225 $\mu$mol) was added in one portion and the resulting mixture was stirred for 5 h at −35 °C. After this time, the reaction was stirred at rt overnight. The reaction was quenched with a solution of tribasic potassium phosphate (401 mg, 1.89 mmol) in water (7 mL), and the layers were separated. The aqueous layer was extracted with $CH_2Cl_2$ (5 mL), and the combining layers were separated. The volatiles were removed under pressure, and the resulting oil was purified by flash column chromatography (hexanes/EtOAc, 100:0 → 100:1) to afford **9a**[10] (137 mg, 0.29 mmol, 64% yield) as a yellow oil: $[\alpha]D^0$ −100.1 (*c* 6.5, EtOH); $^1H$ NMR (360 MHz, $CDCl_3$): $\delta$ 6.55 (br s, 1H, OH-1′/OH-3′), 5.66 (br s, 2H, OH-1′/OH-3′), 5.46 (s, 1H, H-2), 4.53 (s, 1H, H-$10_{trans}$), 4.41 (m, 1H, H-$10_{cis}$), 4.07 (dm, 1H, H-1), 2.92 (m, 2H, H-1″), 2.55 (m, 1H, H-6), 2.22 (m, 1H, H-4), 2.07 (m, 1H, H-4), 1.81−1.74 (m, 2H, H-5), 1.77 (s, 3H, H-7), 1.68 (s, 3H, H-9), 1.58−1.49 (m, 2H, H-2″), 1.43−1.38 (m, 4H, H-3″, H-4″), and 0.92 (m, 3H, H-5″); $^{13}C$ NMR (90 MHz, $CDCl_3$): $\delta$ 151.6 ($C_{3'}$), 150.5 ($C_{1'}$), 147.2 ($C_8$), 139.9 ($C_{5'}$), 139.5 ($C_3$), 123.3 ($C_2$), 115.7 ($C_{2'}$), 111.6 ($C_{10}$), 104.4 ($C_{4'}$, $C_{6'}$), 45.9 ($C_6$), 38.1 ($C_1$), 37.6 ($C_{1''}$), 31.9 ($C_{4''}$), 30.4 ($C_4$), 28.2 ($C_5$), 27.9 ($C_{3''}$), 23.9 ($C_7$), 22.5 ($C_{4''}$), 19.0 ($C_9$), and 14.2 ($C_{5''}$); IR (ATR): 3497, 3395, 2924, 1599, 1429, 1356, and 1248 $cm^{-1}$.

**4,6-Dibromo-5-ethyl-2-[(1*R*,6*R*)-6-isopropenyl-3-methylcyclohex-2-en-1-yl]benzene-1,3-diol (9b).** Compound **9b** was prepared as described for **9a** by using a mixture of **7b** (804 mg, 2.72 mmol), **8** (476 mg, 2.99 mmol), and $MgSO_4$ (818 mg, 6.79 mmol) in dry $CH_2Cl_2$ (70 mL) and *p*-TsOH (258 mg, 1.35 mmol). Yield **9b**: 71% (829 mg, 1.83 mmol) as a yellow oil: $[\alpha]D^0$ −47.3 (*c* 1.1, $CHCl_3$); $^1H$ NMR (360 MHz, $CDCl_3$): $\delta$ 6.57 (br s, 1H, OH-1′/OH-3′), 5.56 (br s, 2H, OH-1′/OH-3′), 5.46 (s, 1H, H-2), 4.53 (s, 1H, H-$10_{trans}$), 4.41 (m, 1H, H-$10_{cis}$), 4.07 (dm, $J_{1,6}$ = 10.2 Hz, 1H, H-1), 2.98 (m, $J_{1'',2''}$ = 7.5 Hz, 2H, H-1″), 2.55 (m, 1H, H-6), 2.22 (m, 1H, H-4), 2.08 (m, 1H, H-4), 1.81−1.74 (m, 2H, H-5), 1.77 (s, 3H, H-7), 1.68 (s, 3H, H-9), and 1.15 (t, $J_{2'',1''}$ = 7.5 Hz, 3H, H-2″); $^{13}C$ NMR (90 MHz, $CDCl_3$): $\delta$ 151.7 ($C_{3'}$), 150.2 ($C_{1'}$), 147.3 ($C_8$), 140.5 ($C_{5'}$), 140.1 ($C_3$), 123.2 ($C_2$), 115.7 ($C_{2'}$), 111.6 ($C_{10}$), 104.3 ($C_{4'}$, $C_{6'}$), 45.9 ($C_6$), 38.0 ($C_1$), 31.2 ($C_5$), 30.4 ($C_4$), 28.2 ($C_{1''}$), 23.9 ($C_7$), 19.0 ($C_9$), and 12.6 ($C_{2''}$); IR (ATR): 3491, 2925, 1737, 1596, 1410, 1244, 1204, and 890 $cm^{-1}$. HRMS ($ESI^-$) calcd for $[C_{18}H_{22}Br_2O_2 - H]^-$ ($[M - H]^-$), 426.9908; found, 426.9918.


https://doi.org/10.1021/acs.jmedchem.1c00561
J. Med. Chem. 2021, 64, 9354−9364

**4,6-Dibromo-2-[(1*R*,6*R*)-6-isopropenyl-3-methylcyclohex-2-en-1-yl]-5-propylbenzene-1,3-diol (9c).** Compound **9c**[50] was prepared as described for **9a** by using a mixture of **7c** (383 g, 1.23 mmol), **8** (242 mg, 1.59 mmol), and $MgSO_4$ (372 mg, 3.09 mmol) in dry $CH_2Cl_2$ (6 mL) and *p*-TsOH (118 mg, 620 μmol). Yield **9c**: 70% (380 mg, 860 μmol) as a yellow oil: $[\alpha]D2^0$ −61.8 (*c* 0.5, $CHCl_3$); $^1H$ NMR (360 MHz, $CDCl_3$): δ 6.56 (br s, 1H, OH-1′/OH-3′), 5.56 (br s, 2H, OH-1′/OH-3′), 5.46 (s, 1H, H-2), 4.53 (s, 1H, H-$10_{trans}$), 4.40 (m, 1H, H-$10_{cis}$), 4.07 (dm, 1H, H-1), 2.90 (m, 2H, H-1″), 2.55 (m, 1H, H-6), 2.20 (m, 1H, H-4), 2.07 (m, 1H, H-4), 1.81−1.74 (m, 2H, H-5), 1.77 (s, 3H, H-7), 1.68 (s, 3H, H-9), 1.58 (sext, $J_{2'',1''/3''}$ = 7.3 Hz, 2H, H-2″), and 1.02 (t, $J_{3'',2''}$ = 7.3 Hz, 3H, H-3″); $^{13}C$ NMR (90 MHz, $CDCl_3$): δ 151.6 ($C_{3'}$), 149.9 ($C_{1'}$), 147.2 ($C_8$), 139.9 ($C_{5'}$), 139.3 ($C_3$), 123.2 ($C_2$), 115.7 ($C_{2'}$), 111.6 ($C_{10}$), 104.5 ($C_{4'}$, $C_{6'}$), 45.9 ($C_6$), 39.5 ($C_{1''}$), 38.0 ($C_1$), 30.4 ($C_4$), 28.2 ($C_5$), 23.9 ($C_7$), 21.7 ($C_{2''}$), 18.9 ($C_9$), and 14.2 ($C_{3''}$); IR (ATR): 3493, 3387, 2925, 1598, 1428, 1325, 1245, 1099, and 889 $cm^{-1}$.

**4,6-Dibromo-5-butyl-2-[(1*R*,6*R*)-6-isopropenyl-3-methylcyclohex-2-en-1-yl]benzene-1,3-diol (9d).** Compound **9d** was prepared as described for **9a** by using a mixture of **7d** (663 mg, 2.05 mmol), **8** (365 mg, 2.39 mmol), and $MgSO_4$ (615 mg, 5.11 mmol) in dry $CH_2Cl_2$ (11 mL) and *p*-TsOH (199 mg, 1.05 mmol). Yield **9d**: 56% (522 mg, 1.14 mmol) as a yellow oil: $[\alpha]D2^0$ −63.1 (*c* 1.9, $CHCl_3$); $^1H$ NMR (360 MHz, $CDCl_3$): δ 6.57 (br s, 1H, OH-1′/OH-3′), 5.56 (br s, 2H, OH-1′/OH-3′), 5.46 (s, 1H, H-2), 4.53 (s, 1H, H-$10_{trans}$), 4.40 (m, 1H, H-$10_{cis}$), 4.06 (dm, 1H, H-1), 2.92 (m, 2H, H-1″), 2.54 (m, 1H, H-6), 2.20 (m, 1H, H-4), 2.09 (m, 1H, H-4), 1.81−1.74 (m, 2H, H-5), 1.77 (s, 3H, H-7), 1.68 (s, 3H, H-9), 1.57−1.42 (m, 4H, H-2″, H-3″), and 0.97 (t, $J_{4'',3''}$ = 7.0 Hz, 3H, H-4″); $^{13}C$ NMR (90 MHz, $CDCl_3$): δ 151.8 ($C_{3'}$), 150.0 ($C_{1'}$), 147.3 ($C_8$), 140.1 ($C_{5'}$), 139.5 ($C_3$), 123.2 ($C_2$), 115.7 ($C_{2'}$), 111.6 ($C_{10}$), 104.4 ($C_{4'}$, $C_{6'}$), 45.9 ($C_6$), 38.1 ($C_1$), 37.4 ($C_{1''}$), 30.4 ($C_4$), 30.4 ($C_{2''}$), 28.2 ($C_5$), 23.9 ($C_7$), 22.9 ($C_{3''}$), 19.0 ($C_9$), and 14.0 ($C_{4''}$); IR (ATR): 3494, 2924, 1600, 1429, 1328, 1247, and 892 $cm^{-1}$. HRMS ($ESI^-$) calcd for $[C_{20}H_{26}Br_2O_2 - H]^-$ ($[M - H]^-$), 455.0221; found, 455.0228.

**4,6-Dibromo-5-hexyl-2-[(1*R*,6*R*)-6-isopropenyl-3-methylcyclohex-2-en-1-yl]benzene-1,3-diol (9e).** Compound **9e** was prepared as described for **9a** by using a mixture of **7e** (629 mg, 1.79 mmol), **8** (299 mg, 1.97 mmol), and $MgSO_4$ (537 mg, 4.47 mmol) in dry $CH_2Cl_2$ (7 mL) and *p*-TsOH (170 mg, 893 μmol). Yield **9e**: 64% (555 mg, 1.14 mmol) as a yellow oil: $[\alpha]D2^0$: −56.5 (*c* 1.6, $CHCl_3$); $^1H$ NMR (360 MHz, $CDCl_3$): δ 6.57 (br s, 1H, OH-1′/OH-3′), 5.67 (br s, 2H, OH-1′/OH-3′), 5.47 (s, 1H, H-2), 4.53 (s, 1H, H-$10_{trans}$), 4.40 (m, 1H, H-$10_{cis}$), 4.06 (dm, 1H, H-1), 2.91 (m, 2H, H-1″), 2.56 (m, 1H, H-6), 2.23 (m, 1H, H-4), 2.08 (m, 1H, H-4), 1.81−1.74 (m, 2H, H-5), 1.77 (s, 3H, H-7), 1.68 (s, 3H, H-9), 1.57−1.49 (m, 2H, H-2″), 1.43−1.34 (m, 6H, H-3″, H-4″, H-5″), and 0.91 (m, 3H, H-6″); $^{13}C$ NMR (90 MHz, $CDCl_3$): δ 151.7 ($C_{3'}$), 150.0 ($C_{1'}$), 147.3 ($C_8$), 140.1 ($C_{5'}$), 139.6 ($C_3$), 123.2 ($C_2$), 115.7 ($C_{2'}$), 111.6 ($C_{10}$), 104.6 ($C_{4'}$, $C_{6'}$), 46.0 ($C_6$), 38.1 ($C_1$), 37.7 ($C_{1''}$), 31.7 ($C_{4''}$), 30.4 ($C_4$), 29.4 ($C_{4''}$), 28.2 ($C_5$), 28.2 ($C_{2''}$), 23.9 ($C_7$), 22.8 ($C_{5''}$), 19.0 ($C_9$), and 14.2 ($C_{6''}$); IR (ATR): 3499, 3394, 2924, 1593, 1428, 1246, and 890 $cm^{-1}$. HRMS ($ESI^-$) calcd for $[C_{22}H_{30}Br_2O_2 - H]^-$ ($[M - H]^-$), 483.0534; found, 483.0537.

**2-[(1*R*,6*R*)-6-Isopropenyl-3-methylcyclohex-2-en-1-yl]-5-pentylbenzene-1,3-diol (1a).** To a solution of **9a** (130 mg, 280 μmol) in methanol (1.5 mL) was added a solution of sodium sulfite (92 mg, 730 μmol) and L-ascorbic acid (7 mg, 40 μmol) in water (1.5 mL). To the pink suspension formed, triethylamine (140 μL, 1.2 mmol) was added in one portion. The resulting mixture was heated to 75 °C for 24 h. After cooling to rt, the reaction mixture was partially concentrated under reduced pressure to remove most of the methanol and volatiles. The pH of the remaining aqueous phase was adjusted to 2 with hydrochloric acid 5% w/w. Hexane (10 mL) was added, and the mixture was stirred for 15 min. The layers were separated, and the aqueous phase was extracted with hexane (2 × 10 mL). The combined organic layers were washed with brine (25 mL), dried over $Na_2SO_4$, and then evaporated under reduced pressure. The obtained oil was purified by flash column chromatography (hexanes/EtOAc, 100:1 → 10:1) to deliver **1a** (38 mg, 12 μmol, 43% yield) as a light-yellow oil: $[\alpha]D2^0$ −122.0 (*c* 1.1, EtOH), −51.3 (*c* 1.7, $CHCl_3$); $^1H$ NMR (400 MHz, $CD_3OD$): δ 6.07 (s, 2H, H-4′, H-6′), 5.28 (s, 1H, H-2), 4.46 (s, 1H, H-$10_{trans}$), 4.42 (m, 1H, H-$10_{cis}$), 3.93 (dm, $J_{1,6}$ = 8.7 Hz, 1H, H-1), 2.89 (m, 1H, H-6), 2.37 (t, $J_{1'',2''}$ = 7.5 Hz, 2H, H-1″), 2.18 (m, 1H, H-4), 1.99 (m, 1H, H-4), 1.74 (m, 2H, H-5), 1.67 (s, 3H, H-7), 1.63 (s, 3H, H-9), 1.53 (quint, $J_{2'',1''/3''}$ = 7.5 Hz, 2H, H-2″), 1.29 (m, 4H, H-3″,H-4″), and 0.89 (t, $J_{5'',4''}$ = 6.9 Hz, 3H, H-5″); $^{13}C$ NMR (100 MHz, $CD_3OD$): δ 157.5 ($C_{3'}$), 150.3 ($C_8$, $C_{1'}$), 142.7 ($C_{5'}$), 134.1 ($C_3$), 127.3 ($C_2$), 115.9 ($C_{2'}$), 110.5 ($C_{10}$), 108.3 ($C_{4'}$, $C_{6'}$), 46.3 ($C_6$), 37.5 ($C_1$), 36.6 ($C_{1''}$), 32.7 ($C_{3''}$), 32.0 ($C_{2''}$), 31.7 ($C_5$), 30.7 ($C_4$), 23.7 ($C_7$), 23.6 ($C_{4''}$), 19.5 ($C_9$), and 14.4 ($C_{5''}$); IR (ATR): 3424, 2926, 1632, 1586, 1447, 1218, and 891 $cm^{-1}$. All spectral data are in agreement with the literature.[12]

**5-Ethyl-2-[(1*R*,6*R*)-6-isopropenyl-3-methylcyclohex-2-en-1-yl]benzene-1,3-diol (1b).** Compound **1b** was prepared as described for **1a** by using a solution of **9b** (709 mg, 1.65 mmol) in MeOH (7 mL), a solution of $Na_2SO_3$ (551 g, 4.37 mmol) and L-ascorbic acid (43.6 mg, 250 μmol) in $H_2O$ (7 mL), and $Et_3N$ (830 μL, 5.94 mmol). Yield **1b**: 63% (282 mg, 1.04 mmol) as a light-brown oil: $[\alpha]D2^0$ −86.9 (*c* 1.9, $CHCl_3$); $^1H$ NMR (400 MHz, $CD_3OD$): δ 6.10 (s, 2H, H-4′, H-6′), 5.28 (s, 1H, H-2), 4.48 (s, 1H, H-$10_{trans}$), 4.44 (m, 1H, H-$10_{cis}$), 3.93 (dm, $J_{1,6}$ = 8.7 Hz, 1H, H-1), 2.92 (m, 1H, H-6), 2.42 (q, $J_{1'',2''}$ = 7.6 Hz, 2H, H-1″), 2.18 (m, 1H, H-4), 1.99 (m, 1H, H-4), 1.74 (m, 2H, H-5), 1.68 (s, 3H, H-7), 1.64 (s, 3H, H-9), and 1.15 (t, $J_{2'',1''}$ = 7.6 Hz, 3H, H-2″); $^{13}C$ NMR (100 MHz, $CD_3OD$): δ 157.5 ($C_{3'}$), 150.3 ($C_8$, $C_{1'}$), 144.1 ($C_{5'}$), 134.1 ($C_3$), 127.3 ($C_2$), 115.9 ($C_{2'}$), 110.5 ($C_{10}$), 107.7 ($C_{4'}$, $C_{6'}$), 46.3 ($C_6$), 37.4 ($C_1$), 31.7 ($C_5$), 30.8 ($C_4$), 29.5 ($C_{1''}$), 23.7 ($C_7$), 19.5 ($C_9$), and 15.8 ($C_{2''}$); IR (ATR): 3405, 2925, 1628, 1582, 1439, 1215, and 888 $cm^{-1}$. HRMS ($ESI^+$) calcd for $[C_{18}H_{24}O_2 + H]^+$ ($[M + H]^+$), 273.1855; found, 273.1849.

**2-[(1*R*,6*R*)-6-Isopropenyl-3-methylcyclohex-2-en-1-yl]-5-propylbenzene-1,3-diol (1c).** Compound **1c**[13] was prepared as described for **1a** by using a solution of **9c** (321 mg, 723 μmol) in MeOH (4 mL), a solution of $Na_2SO_3$ (262 g, 2.26 mmol) and L-ascorbic acid (37 mg, 210 μmol) in $H_2O$ (4 mL), and $Et_3N$ (410 μL, 2.94 mmol). Yield **1c**: 50% (103 mg, 360 μmol) as a brown oil: $[\alpha]D2^0$ −138.3 (*c* 2.3, EtOH), −72.23. (*c* 0.5, $CHCl_3$); $^1H$ NMR (400 MHz, $CD_3OD$): δ 6.09 (s, 2H, H-4′, H-6′), 5.30 (s, 1H, H-2), 4.47 (s, 1H, H-$10_{trans}$), 4.44 (m, 1H, H-$10_{cis}$), 3.94 (dm, $J_{1,6}$ = 8.6 Hz, 1H, H-1), 2.90 (m, 1H, H-6), 2.36 (t, $J_{1'',2''}$ = 7.5 Hz, 2H, H-1″), 2.18 (m, 1H, H-4), 1.99 (m, 1H, H-4), 1.74 (m, 2H, H-5), 1.68 (s, 3H, H-7), 1.64 (s, 3H, H-9), 1.57 (sext, $J_{2'',1''/3''}$ = 7.5 Hz, 2H, H-2″), and 0.90 (t, $J_{3'',2''}$ = 7.5 Hz, 3H, H-3″); $^{13}C$ NMR (100 MHz, $CD_3OD$): δ 157.4 ($C_{3'}$), 150.2 ($C_8$, $C_{1'}$), 142.4 ($C_{5'}$), 134.3 ($C_3$), 127.2 ($C_2$), 115.9 ($C_{2'}$), 110.5 ($C_{10}$), 108.3 ($C_{4'}$, $C_{6'}$), 46.3 ($C_6$), 38.8 ($C_{1''}$), 37.4 ($C_1$), 31.6 ($C_5$), 30.7 ($C_4$), 25.4 ($C_{2''}$), 23.7 ($C_7$), 19.5 ($C_9$), and 14.2 ($C_{3''}$); IR (ATR): 3412, 2924, 1629, 1534, 1443, 1217, and 889 $cm^{-1}$. HRMS ($ESI^+$) calcd for $[C_{19}H_{26}O_2 + H]^+$ ($[M + H]^+$), 287.2011; found, 287.2009.

**5-Butyl-2-[(1*R*,6*R*)-6-isopropenyl-3-methylcyclohex-2-en-1-yl]benzene-1,3-diol (1d).** Compound **1d**[14] was prepared as described for **1a** by using a solution of **9d** (292 mg, 637 μmol) in MeOH (4 mL), a solution of $Na_2SO_3$ (229 mg, 1.97 mmol) and L-ascorbic acid (31 mg, 176 μmol) in $H_2O$ (4 mL), and $Et_3N$ (350 μL, 2.51 mmol). Yield **1d**: 56% (108 mg, 360 μmol) as a brown oil: $[\alpha]D2^0$ −56.1 (*c* 1.0, $CHCl_3$); $^1H$ NMR (400 MHz, $CD_3OD$): δ 6.08 (s, 2H, H-4′, H-6′), 5.28 (s, 1H, H-2), 4.47 (s, 1H, H-$10_{trans}$), 4.43 (m, 1H, H-$10_{cis}$), 3.93 (dm, $J_{1,6}$ = 8.6 Hz, 1H, H-1), 2.91 (m, 1H, H-6), 2.39 (t, $J_{1'',2''}$ = 7.6 Hz, 2H, H-1″), 2.18 (m, 1H, H-4), 1.99 (m, 1H, H-4), 1.74 (m, 2H, H-5), 1.68 (s, 3H, H-7), 1.64 (s, 3H, H-9), 1.53 (quint, $J_{2'',1''/3''}$ = 7.6 Hz, 2H, H-2″), 1.34 (sext, $J_{3'',2''/4''}$ = 7.4 Hz, 2H, H-2″), and 0.92 (t, $J_{4'',3''}$ = 7.4 Hz, 3H, H-4″); $^{13}C$ NMR (100 MHz, $CD_3OD$): δ 157.5 ($C_{3'}$), 150.3 ($C_8$, $C_{1'}$), 142.6 ($C_{5'}$), 134.0 ($C_3$), 127.2 ($C_2$), 115.9 ($C_{2'}$), 110.5 ($C_{10}$), 108.3 ($C_{4'}$, $C_{6'}$), 46.3 ($C_6$), 37.4 ($C_1$), 36.3 ($C_{1''}$), 34.6 ($C_{2''}$), 31.7 ($C_5$), 30.8 ($C_4$), 23.7 ($C_7$), 23.4 ($C_{3''}$), 19.5 ($C_9$), and 14.3 ($C_{4''}$); IR (ATR): 3429, 2925, 1629, 1583, 1441, 1213, and 1025 $cm^{-1}$. HRMS ($ESI^+$) calcd for $[C_{20}H_{28}O_2 + H]^+$ ($[M + H]^+$), 301.2168; found, 301.2163.


https://doi.org/10.1021/acs.jmedchem.1c00561
J. Med. Chem. 2021, 64, 9354−9364

**5-Hexyl-2-[(1*R*,6*R*)-6-isopropenyl-3-methylcyclohex-2-en-1-yl]benzene-1,3-diol (1e).** Compound **1e** was prepared as described for **1a** by using a solution of **9e** (26 mg, 53 μmol) in MeOH (1 mL), a solution of $Na_2SO_3$ (19 mg, 167 μmol) and L-ascorbic acid (4 mg, 14 μmol) in $H_2O$ (1 mL), and $Et_3N$ (30 μL, 214 μmol). Yield **1e**: 63% (11 mg, 33 μmol) as a brown oil: $[\alpha]D2^0$: −50.2 (*c* 0.5, $CHCl_3$); $^1H$ NMR (400 MHz, $CD_3OD$): δ 6.09 (s, 2H, H-4′, H-6′), 5.30 (s, 1H, H-2), 4.47 (s, 1H, H-$10_{trans}$), 4.43 (m, 1H, H-$10_{cis}$), 3.94 (dm, $J_{1,6}$ = 8.7 Hz, 1H, H-1), 2.89 (m, 1H, H-6), 2.38 (t, $J_{1'',2''}$ = 7.6 Hz, 2H, H-1″), 2.18 (m, 1H, H-4), 1.99 (m, 1H, H-4), 1.74 (m, 2H, H-5), 1.68 (s, 3H, H-7), 1.64 (s, 3H, H-9), 1.54 (m, 2H, H-2″), 1.30 (m, 6H, H-3″, H-4″, H-5″), and 0.89 (m, 3H, H-6″); $^{13}C$ NMR (100 MHz, $CD_3OD$): δ 157.4 ($C_{3'}$), 150.2 ($C_8$, $C_{1'}$), 142.6 ($C_{5'}$), 134.3 ($C_3$), 127.3 ($C_2$), 115.8 ($C_{2'}$), 110.6 ($C_{10}$), 108.3 ($C_{4'}$, $C_{6'}$), 46.3 ($C_6$), 37.4 ($C_1$), 36.6 ($C_{1''}$), 32.9 ($C_{4''}$), 32.3 ($C_{3''}$), 31.7 ($C_5$), 30.6 ($C_4$), 30.0 ($C_{2''}$), 23.8 ($C_{5''}$), 23.7 ($C_7$), 19.5 ($C_9$), and 14.5 ($C_{6''}$); IR (ATR): 3438, 2923, 1629, 1583, 1444, 1217, 1027, and 888 $cm^{-1}$. HRMS ($ESI^+$) calcd for $[C_{22}H_{32}O_2 + H]^+$ ($[M + H]^+$), 329.2481; found, 329.2477.

**cAMP Determination Assays.** Determination of cAMP levels in HEK-293T cells transiently expressing $CB_2R$ (1 μg of cDNA) was performed using the Lance-Ultra cAMP kit (PerkinElmer). 2 h before initiating the experiment, the medium was substituted by a serum-free medium. Then, transfected cells were dispensed in white 384-well microplates at a density of 3000 cells per well and incubated for 15 min at rt with compounds, followed by 15 min incubation with forskolin, and 1 h more with homogeneous time-resolved fluorescence (HTRF) assay reagents. Fluorescence at 665 nm was analyzed on a PHERAstar Flagship microplate reader equipped with an HTRF optical module (BMG Labtech). Data analysis was made based on the fluorescence ratio emitted by the labeled cAMP probe (665 nm) over the light emitted by the europium cryptate-labeled anti-cAMP antibody (620 nm). A standard curve was used to calculate cAMP concentration. Forskolin-stimulated cAMP levels were normalized to 100%

**ERK1/2 Phosphorylation Assays.** HEK-293T cells were grown on transparent Biocat poly-D-lysine 96-well plates (Deltalab) and kept at an incubator for 24 h. Then, cells were transiently transfected with 1 μg of cDNA coding for $CB_2R$ or mutant receptors and incubated for 48 h at 37 °C in a 5% $CO_2$ humid atmosphere. 2 h before initiating the experiment, the medium was substituted by a serum-free medium. Cells were stimulated at 25 °C for 7 min with vehicles or agonists in the serum-free Dulbecco's modified Eagle's medium. After that, cells were washed twice with cold phosphate-buffered saline before the addition of lysis buffer (30 μL/well) and incubated for 15 min at 25 °C on a Heidolph Titramax 100 shaker. 10 μl of each cell lysate was transferred to white ProxiPlate 384-well microplates (PerkinElmer; Waltham, MA, USA). ERK1/2 phosphorylation was determined using an AlphaScreenSureFire kit (PerkinElmer, Waltham, MA, US): 5 μL/well of acceptor beads was added. Plates, protected from light, were incubated for 2 h at 25 °C. Finally, 5 μL/well of donor beads was added and plates, protected from light, were incubated for 2 h before analysis. Fluorescence was determined using an EnSpire Multimode Plate Reader (PerkinElmer, Waltham, MA, USA). The value of reference (100%) was that achieved in the absence of any treatment (basal). The effect of ligands was given in percentage with respect to the basal value.

**Dynamic Mass Redistribution Assays.** Cell mass redistribution induced upon receptor activation was detected by illuminating with polychromatic light the underside of a biosensor and measuring the changes in the wavelength of the reflected monochromatic light that is a sensitive function of the index of refraction. The magnitude of the wavelength shift (in picometers) is directly proportional to the amount of mass redistribution. 48 h before the assay, HEK-293T cells were transiently transfected with 1 μg of cDNA coding for $CB_2R$ or mutant receptors. HEK-293T cells were seeded in 384-well sensor microplates to obtain 70−80% confluent monolayers constituted by approximately 10,000 cells/well. Prior to the assay, cells were washed twice with an assay buffer (HBSS with 20 mM HEPES, pH 7.15, and 1% BSA) (SigmaAldrich, St. Louis, MO, US) and incubated for 2 h with an assay buffer containing 0.1% DMSO (24 °C, 30 μL/well). Hereafter, the sensor plate was scanned, and a baseline optical signature was recorded for 10 min before adding 10 μL of the selective antagonists for 30 min, followed by the addition of 10 μL of the selective agonists; all test compounds were diluted in the assay buffer. Then, DMR responses were monitored for at least 5000 s in an EnSpire Multimode Plate Reader (PerkinElmer, Waltham, MA, USA) by a label-free technology. Results were analyzed using EnSpire Workstation Software v 4.10.

**Molecular Docking and MD Simulations.** The $CB_2R$-AM12033-$G_i$ cryo-EM structure (PDB id 6KPF)[18] (missing residues 55−181 and 233−239 of $\alpha_i$- were built from the $CB_2R$-WIN55, 212-2-$G_i$ structure, 6PT0,[17] using MODELLER v9.25) was used in docking studies and MD simulations. JWH-133 and CBD were docked into the orthosteric binding cavity (Figure S1), and CBD, PAM **1c**, and NAM **1e** were docked into the allosteric binding cavity (Figure S4) using the Molecular Operating Environment software (Chemical Computing Group Inc., Montreal, Quebec, Canada). These structures were embedded in a lipid bilayer box, constructed using PACKMOL-memgen,[51] containing 1-palmitoyl-2-oleoyl-*sn*-glycero-3-phosphocholine, cholesterol , water molecules (TIP3P), and monoatomic $Na^+$ and $Cl^-$ ions (see Figure S3 for details). MD simulation of these systems was performed with GROMACS 2019[52] (Figures S3 and S5).

## ■ ASSOCIATED CONTENT

### Supporting Information

The Supporting Information is available free of charge at https://pubs.acs.org/doi/10.1021/acs.jmedchem.1c00561.

Computer models of JWH-133 and CBD bound to the orthosteric site of $CB_2R$; superimposition of the computer model of $CB_2R$ in complex with JWH-133 to the crystal structure of $CB_1R$ in complex with AM6538; MD simulations of JWH-133, JWH-133 + CBD, JWH-133 + **1c**, and JWH-133 + **1e** bound to the $CB_2R$-$G_i$ complex; docking of CBD to the $CB_2R$-$G_i$ complex; $^1H$ and $^{13}C$ NMR spectra of the new compounds; and 1D $^1H$ NMR (qHNMR) experiments of compounds **1a−e** (PDF)

SMILES of JWH-133 and compounds **1a−e** (CSV)

Molecular complex data of $CB_2R$ + JWH-133 + CBD (PDB)

## ■ AUTHOR INFORMATION


### Corresponding Authors

**Ramon Alibés** − *Departament de Química, Universitat Autònoma de Barcelona, Bellaterra 08193, Barcelona, Spain;* orcid.org/0000-0002-7997-2691; Email: Ramon.Alibes@uab.cat

**Leonardo Pardo** − *Laboratory of Computational Medicine, Biostatistics Unit, Faculty of Medicine, Universitat Autònoma Barcelona, Bellaterra 08193, Barcelona, Spain;* orcid.org/0000-0003-1778-7420; Email: Leonardo.Pardo@uab.es

**Rafael Franco** − *Centro de Investigación en Red, Enfermedades Neurodegenerativas (CIBERNED), Instituto de Salud Carlos III, 28031 Madrid, Spain; Department of Biochemistry and Molecular Biomedicine, Faculty of Biology, Universitat de Barcelona, 08028 Barcelona, Spain;* orcid.org/0000-0003-2549-4919; Email: rfranco123@gmail.com, rfranco@ub.edu

### Authors

**Gemma Navarro** − *Department of Biochemistry and Physiology, Faculty of Pharmacy and Food Sciences, Universitat de Barcelona, 08028 Barcelona, Spain; Centro de*




https://doi.org/10.1021/acs.jmedchem.1c00561
J. Med. Chem. 2021, 64, 9354−9364

*Investigación en Red, Enfermedades Neurodegenerativas (CIBERNED), Instituto de Salud Carlos III, 28031 Madrid, Spain*

**Angel Gonzalez** − *Laboratory of Computational Medicine, Biostatistics Unit, Faculty of Medicine, Universitat Autònoma Barcelona, Bellaterra 08193, Barcelona, Spain*

**Adrià Sánchez-Morales** − *Departament de Química, Universitat Autònoma de Barcelona, Bellaterra 08193, Barcelona, Spain*

**Nil Casajuana-Martin** − *Laboratory of Computational Medicine, Biostatistics Unit, Faculty of Medicine, Universitat Autònoma Barcelona, Bellaterra 08193, Barcelona, Spain*

**Marc Gómez-Ventura** − *Departament de Química, Universitat Autònoma de Barcelona, Bellaterra 08193, Barcelona, Spain*

**Arnau Cordomí** − *Laboratory of Computational Medicine, Biostatistics Unit, Faculty of Medicine, Universitat Autònoma Barcelona, Bellaterra 08193, Barcelona, Spain*

**Félix Busqué** − *Departament de Química, Universitat Autònoma de Barcelona, Bellaterra 08193, Barcelona, Spain*

Complete contact information is available at: https://pubs.acs.org/10.1021/acs.jmedchem.1c00561

### Author Contributions

G.N., A.G., and A.S.M. authors contributed equally. G.N., A.C., L.P., and R.F. devised the project concept and designed experiments. A.G. and N.C.M. contributed with computational simulations. A.S.M. and M.G.V. synthesized compounds, supervised by F.B. and R.A. G.N. performed the biochemical and molecular assays. R.A., L.P., and R.F. wrote the paper with contributions from all other authors. All authors contributed to the data analysis and have given approval to the final version of the manuscript.

### Funding

We acknowledge the financial support from the Spanish Ministry of Economy and Innovation with FEDER funds (projects SAF2017-84117-R, RTI2018-098830-B-I00, PID2019-106403RB-I00, and PID2019-109240RB-I00).

### Notes

The authors declare no competing financial interest.

## ■ ACKNOWLEDGMENTS

A.S.M. acknowledges the Universitat Autònoma de Barcelona for its predoctoral grant.

## ■ ABBREVIATIONS

GPCR, G-protein-coupled receptor; $CB_2R$, cannabinoid $CB_2$ receptor; $CB_1R$, cannabinoid $CB_1$ receptor; CBD, cannabidiol; THC, Δ9-tetrahydrocannabinol; NAM, negative allosteric modulator; PAM, positive allosteric modulator; MD, molecular dynamic; TM, transmembrane helix

## ■ REFERENCES

(1) Iffland, K.; Grotenhermen, F. An Update on Safety and Side Effects of Cannabidiol: A Review of Clinical Data and Relevant Animal Studies. *Cannabis Cannabinoid Res.* **2017**, *2*, 139−154.

(2) White, C. M. A Review of Human Studies Assessing Cannabidiol's (CBD) Therapeutic Actions and Potential. *J. Clin. Pharmacol.* **2019**, *59*, 923−934.

(3) Giacoppo, S.; Bramanti, P.; Mazzon, E. Sativex in the Management of Multiple Sclerosis-Related Spasticity: An Overview of the last Decade of Clinical Evaluation. *Mult. Scler. Relat. Disord.* **2017**, *17*, 22−31.

(4) Devinsky, O.; Patel, A. D.; Cross, J. H.; Villanueva, V.; Wirrell, E. C.; Privitera, M.; Greenwood, S. M.; Roberts, C.; Checketts, D.; VanLandingham, K. E.; Zuberi, S. M.; Group, G. S. Effect of Cannabidiol on Drop Seizures in the Lennox-Gastaut Syndrome. *N. Engl. J. Med.* **2018**, *378*, 1888−1897.

(5) Billakota, S.; Devinsky, O.; Marsh, E. Cannabinoid Therapy in Epilepsy. *Curr. Opin. Neurol.* **2019**, *32*, 220−226.

(6) Fasinu, P. S.; Phillips, S.; ElSohly, M. A.; Walker, L. A. Current Status and Prospects for Cannabidiol Preparations as New Therapeutic Agents. *Pharmacotherapy* **2016**, *36*, 781−796.

(7) Morales, P.; Reggio, P. H. CBD: A New Hope? *ACS Med. Chem. Lett.* **2019**, *10*, 694−695.

(8) Ibeas Bih, C.; Chen, T.; Nunn, A. V. W.; Bazelot, M.; Dallas, M.; Whalley, B. J. Molecular Targets of Cannabidiol in Neurological Disorders. *Neurotherapeutics* **2015**, *12*, 699−730.

(9) Morales, P.; Reggio, P. H.; Jagerovic, N. An Overview on Medicinal Chemistry of Synthetic and Natural Derivatives of Cannabidiol. *Front. Pharmacol.* **2017**, *8*, 422.

(10) Thomas, A.; Baillie, G. L.; Phillips, A. M.; Razdan, R. K.; Ross, R. A.; Pertwee, R. G. Cannabidiol Displays Unexpectedly high Potency as an Antagonist of CB1 and CB2 Receptor Agonists in vitro. *Br. J. Pharmacol.* **2007**, *150*, 613−623.

(11) McPartland, J. M.; Duncan, M.; Di Marzo, V.; Pertwee, R. G. Are Cannabidiol and Delta(9)-tetrahydrocannabivarin Negative Modulators of the Endocannabinoid System? A Systematic Review. *Br. J. Pharmacol.* **2015**, *172*, 737−753.

(12) Laprairie, R. B.; Bagher, A. M.; Kelly, M. E. M.; Denovan-Wright, E. M. Cannabidiol is a Negative Allosteric Modulator of the Cannabinoid CB1 Receptor. *Br. J. Pharmacol.* **2015**, *172*, 4790−4805.

(13) Martínez-Pinilla, E.; Varani, K.; Reyes-Resina, I.; Angelats, E.; Vincenzi, F.; Ferreiro-Vera, C.; Oyarzabal, J.; Canela, E. I.; Lanciego, J. L.; Nadal, X.; Navarro, G.; Borea, P. A.; Franco, R. Binding and Signaling Studies Disclose a Potential Allosteric Site for Cannabidiol in Cannabinoid CB2 Receptors. *Front. Pharmacol.* **2017**, *8*, 744.

(14) McPartland, J. M.; Glass, M.; Pertwee, R. G. Meta-analysis of Cannabinoid Ligand Binding Affinity and Receptor Distribution: Interspecies Differences. *Br. J. Pharmacol.* **2007**, *152*, 583−593.

(15) Navarro, G.; Reyes-Resina, I.; Rivas-Santisteban, R.; Sánchez de Medina, V.; Morales, P.; Casano, S.; Ferreiro-Vera, C.; Lillo, A.; Aguinaga, D.; Jagerovic, N.; Nadal, X.; Franco, R. Cannabidiol Skews Biased Agonism at Cannabinoid CB1 and CB2 Receptors with smaller Effect in CB1-CB2 Heteroreceptor Complexes. *Biochem. Pharmacol.* **2018**, *157*, 148−158.

(16) Li, X.; Hua, T.; Vemuri, K.; Ho, J.-H.; Wu, Y.; Wu, L.; Popov, P.; Benchama, O.; Zvonok, N.; Locke, K. a.; Qu, L.; Han, G. W.; Iyer, M. R.; Cinar, R.; Coffey, N. J.; Wang, J.; Wu, M.; Katritch, V.; Zhao, S.; Kunos, G.; Bohn, L. M.; Makriyannis, A.; Stevens, R. C.; Liu, Z.-J. Crystal Structure of the Human Cannabinoid Receptor CB2. *Cell* **2019**, *176*, 459−467.

(17) Xing, C.; Zhuang, Y.; Xu, T.-H.; Feng, Z.; Zhou, X. E.; Chen, M.; Wang, L.; Meng, X.; Xue, Y.; Wang, J.; Liu, H.; McGuire, T. F.; Zhao, G.; Melcher, K.; Zhang, C.; Xu, H. E.; Xie, X.-Q. Cryo-EM Structure of the Human Cannabinoid Receptor CB2-Gi Signaling Complex. *Cell* **2020**, *180*, 645−654.

(18) Hua, T.; Li, X.; Wu, L.; Iliopoulos-Tsoutsouvas, C.; Wang, Y.; Wu, M.; Shen, L.; Brust, C. A.; Nikas, S. P.; Song, F.; Song, X.; Yuan, S.; Sun, Q.; Wu, Y.; Jiang, S.; Grim, T. W.; Benchama, O.; Stahl, E. L.; Zvonok, N.; Zhao, S.; Bohn, L. M.; Makriyannis, A.; Liu, Z.-J. Activation and Signaling Mechanism Revealed by Cannabinoid Receptor-Gi Complex Structures. *Cell* **2020**, *180*, 655−665.

(19) Polini, B.; Cervetto, C.; Carpi, S.; Pelassa, S.; Gado, F.; Ferrisi, R.; Bertini, S.; Nieri, P.; Marcoli, M.; Manera, C. Positive Allosteric Modulation of CB1 and CB2 Cannabinoid Receptors Enhances the Neuroprotective Activity of a Dual CB1R/CB2R Orthosteric Agonist. *Life* **2020**, *10*, 333.

(20) Petrucci, V.; Chicca, A.; Glasmacher, S.; Paloczi, J.; Cao, Z.; Pacher, P.; Gertsch, J. Pepcan-12 (RVD-hemopressin) is a CB2 Receptor Positive Allosteric Modulator Constitutively Secreted by Adrenals and in Liver upon Tissue Damage. *Sci. Rep.* **2017**, *7*, 9560.

(21) Gado, F.; Di Cesare Mannelli, L.; Lucarini, E.; Bertini, S.; Cappelli, E.; Digiacomo, M.; Stevenson, L. A.; Macchia, M.; Tuccinardi, T.; Ghelardini, C.; Pertwee, R. G.; Manera, C. Identification of the First Synthetic Allosteric Modulator of the CB2 Receptors and Evidence of Its Efficacy for Neuropathic Pain Relief. *J. Med. Chem.* **2019**, *62*, 276−287.
(22) Schröder, R.; Schmidt, J.; Blättermann, S.; Peters, L.; Janssen, N.; Grundmann, M.; Seemann, W.; Kaufel, D.; Merten, N.; Drewke, C.; Gomeza, J.; Milligan, G.; Mohr, K.; Kostenis, E. Applying Label-Free Dynamic Mass Redistribution Technology to Frame Signaling of G protein-Coupled Receptors Noninvasively in Living Cells. *Nat. Protoc.* **2011**, *6*, 1748−1760.
(23) González, A.; Perez-Acle, T.; Pardo, L.; Deupi, X. Molecular Basis of Ligand Dissociation in beta-Adrenergic Receptors. *PLoS One* **2011**, *6*, No. e23815.
(24) Kruse, A. C.; Ring, A. M.; Manglik, A.; Hu, J.; Hu, K.; Eitel, K.; Hübner, H.; Pardon, E.; Valant, C.; Sexton, P. M.; Christopoulos, A.; Felder, C. C.; Gmeiner, P.; Steyaert, J.; Weis, W. I.; Garcia, K. C.; Wess, J.; Kobilka, B. K. Activation and Allosteric Modulation of a Muscarinic Acetylcholine Receptor. *Nature* **2013**, *504*, 101−106.
(25) Audet, M.; Stevens, R. C. Emerging Structural Biology of Lipid G protein-Coupled Receptors. *Protein Sci.* **2019**, *28*, 292−304.
(26) Stanley, N.; Pardo, L.; Fabritiis, G. D. The pathway of Ligand entry from the Membrane Bilayer to a Lipid G protein-Coupled Receptor. *Sci. Rep.* **2016**, *6*, 22639.
(27) Morales, P.; Navarro, G.; Gómez-Autet, M.; Redondo, L.; Fernández-Ruiz, J.; Pérez-Benito, L.; Cordomí, A.; Pardo, L.; Franco, R.; Jagerovic, N. Discovery of Homobivalent Bitopic Ligands of the Cannabinoid CB2 Receptor. *Chemistry* **2020**, *26*, 15839−15842.
(28) Hua, T.; Vemuri, K.; Pu, M.; Qu, L.; Han, G. W.; Wu, Y.; Zhao, S.; Shui, W.; Li, S.; Korde, A.; Laprairie, R. B.; Stahl, E. L.; Ho, J.-H.; Zvonok, N.; Zhou, H.; Kufareva, I.; Wu, B.; Zhao, Q.; Hanson, M. A.; Bohn, L. M.; Makriyannis, A.; Stevens, R. C.; Liu, Z.-J. Crystal Structure of the Human Cannabinoid Receptor CB1. *Cell* **2016**, *167*, 750−762.
(29) Saleh, N.; Hucke, O.; Kramer, G.; Schmidt, E.; Montel, F.; Lipinski, R.; Ferger, B.; Clark, T.; Hildebrand, P. W.; Tautermann, C. S. Multiple Binding Sites Contribute to the Mechanism of Mixed Agonistic and Positive Allosteric Modulators of the Cannabinoid CB1 Receptor. *Angew. Chem., Int. Ed. Engl.* **2018**, *57*, 2580−2585.
(30) Solórzano, R.; Tort, O.; García-Pardo, J.; Escribà, T.; Lorenzo, J.; Arnedo, M.; Ruiz-Molina, D.; Alibés, R.; Busqué, F.; Novio, F. Versatile iron−catechol-based Nanoscale Coordination Polymers with Antiretroviral Ligand Functionalization and their use as Efficient Carriers in HIV/AIDS Therapy. *Biomater. Sci.* **2019**, *7*, 178−186.
(31) Zysman-Colman, E.; Arias, K.; Siegel, J. S. Synthesis of Arylbromides from Arenes and N-bromosuccinimide (NBS) in Acetonitrile-A convenient Method for Aromatic Bromination. *Can. J. Chem.* **2009**, *87*, 440−447.
(32) Kinney, W. A.; McDonnell, M. E.; Zhong, H. M.; Liu, C.; Yang, L.; Ling, W.; Qian, T.; Chen, Y.; Cai, Z.; Petkanas, D.; Brenneman, D. E. Discovery of KLS-13019, a Cannabidiol-Derived Neuroprotective Agent, with Improved Potency, Safety, and Permeability. *ACS Med. Chem. Lett.* **2016**, *7*, 424−428.
(33) Tomanová, M.; Jedinák, L.; Cankař, P. Reductive Dehalogenation and Dehalogenative Sulfonation of Phenols and Heteroaromatics with Sodium Sulfite in an Aqueous Medium. *Green Chem.* **2019**, *21*, 2621−2628.
(34) McAllister, S. D.; Hurst, D. P.; Barnett-Norris, J.; Lynch, D.; Reggio, P. H.; Abood, M. E. Structural Mimicry in class A G protein-Coupled Receptor Rotamer Toggle Switches: the importance of the F3.36(201)/W6.48(357) Interaction in Cannabinoid CB1 Receptor Activation. *J. Biol. Chem.* **2004**, *279*, 48024−48037.
(35) Krishna Kumar, K.; Shalev-Benami, M.; Robertson, M. J.; Hu, H.; Banister, S. D.; Hollingsworth, S. A.; Latorraca, N. R.; Kato, H. E.; Hilger, D.; Maeda, S.; Weis, W. I.; Farrens, D. L.; Dror, R. O.; Malhotra, S. V.; Kobilka, B. K.; Skiniotis, G. Structure of a Signaling Cannabinoid Receptor 1-G Protein Complex. *Cell* **2019**, *176*, 448−458.
(36) Pellissier, L. P.; Sallander, J.; Campillo, M.; Gaven, F.; Queffeulou, E.; Pillot, M.; Dumuis, A.; Claeysen, S.; Bockaert, J.; Pardo, L. Conformational Toggle Switches implicated in Basal Constitutive and Agonist-Induced Activated States of 5-hydroxytryptamine-4 Receptors. *Mol. Pharmacol.* **2009**, *75*, 982−990.
(37) Ersoy, B. A.; Pardo, L.; Zhang, S.; Thompson, D. A.; Millhauser, G.; Govaerts, C.; Vaisse, C. Mechanism of N-terminal Modulation of Activity at the Melanocortin-4 Receptor GPCR. *Nat. Chem. Biol.* **2012**, *8*, 725−730.
(38) Pérez-Benito, L.; Doornbos, M. L. J.; Cordomí, A.; Peeters, L.; Lavreysen, H.; Pardo, L.; Tresadern, G. Molecular Switches of Allosteric Modulation of the Metabotropic Glutamate 2 Receptor. *Structure* **2017**, *25*, 1153−1162.
(39) Navarro, G.; Gonzalez, A.; Campanacci, S.; Rivas-Santisteban, R.; Reyes-Resina, I.; Casajuana-Martin, N.; Cordomí, A.; Pardo, L.; Franco, R. Experimental and Computational Analysis of Biased Agonism on full-length and a C-terminally Truncated Adenosine A2A Receptor. *Comput. Struct. Biotechnol. J.* **2020**, *18*, 2723−2732.
(40) Dethe, D. H.; Erande, R. D.; Mahapatra, S.; Das, S.; Kumar, B. V. Protecting Group free Enantiospecific Total Syntheses of Structurally Diverse Natural Products of the Tetrahydrocannabinoid family. *Chem. Commun.* **2015**, *51*, 2871−2873.
(41) Dialer, L.; Petrovic, L.; Weigl, U. Process for the Production of Cannabidiol and delta-9-tetrahydrocannabinol. WO 2017011210 A1, 2017.
(42) Troupiotis-Tsaïlaki, A.; Zachmann, J.; González-Gil, I.; Gonzalez, A.; Ortega-Gutiérrez, S.; López-Rodríguez, M. L.; Pardo, L.; Govaerts, C. Ligand Chain length Drives Activation of Lipid G protein-Coupled Receptors. *Sci. Rep.* **2017**, *7*, 2020.
(43) https://getcontacts.github.io/ (accessed Jan 2021).
(44) Dhopeshwarkar, A.; Mackie, K. CB2 Cannabinoid Receptors as a Therapeutic Target-what does the Future hold? *Mol. Pharmacol.* **2014**, *86*, 430−437.
(45) Slivicki, R. A.; Xu, Z.; Kulkarni, P. M.; Pertwee, R. G.; Mackie, K.; Thakur, G. A.; Hohmann, A. G. Positive Allosteric Modulation of Cannabinoid Receptor Type 1 Suppresses Pathological Pain Without Producing Tolerance or Dependence. *Biol. Psychiatry* **2018**, *84*, 722−733.
(46) Cabañero, D.; Ramírez-López, A.; Drews, E.; Schmöle, A.; Otte, D. M.; Wawrzczak-Bargiela, A.; Huerga Encabo, H.; Kummer, S.; Ferrer-Montiel, A.; Przewlocki, R.; Zimmer, A.; Maldonado, R. Protective Role of Neuronal and Lymphoid Cannabinoid CB2 Receptors in Neuropathic Pain. *Elife* **2020**, *9*, No. e55582.
(47) Lesch, B.; Toräng, J.; Nieger, M.; Bräse, S. The Diels-Alder Approach towards Cannabinoids. *Synthesis* **2005**, 1888−1900.
(48) Roberts, J. C.; Pincock, J. A. Methoxy-substituted Stilbenes, Styrenes, and 1-arylpropenes: Photophysical Properties and Photoadditions of Alcohols. *J. Org. Chem.* **2006**, *71*, 1480−1492.
(49) Poldy, J.; Peakall, R.; Barrow, R. A. Synthesis of Chiloglottones-semiochemicals from Sexually Deceptive Orchids and their Ollinators. *Org. Biomol. Chem.* **2009**, *7*, 4296−4300.
(50) Usami, N.; Okuda, T.; Yoshida, H.; Kimura, T.; Watanabe, K.; Yoshimura, H.; Yamamoto, I. Synthesis and Pharmacological Evaluation in Mice of Halogenated Cannabidiol Derivatives. *Chem. Pharm. Bull.* **1991**, *47*, 1641−1645.
(51) Schott-Verdugo, S.; Gohlke, H. PACKMOL-Memgen: A Simple-To-Use, Generalized Workflow for Membrane-Protein-Lipid-Bilayer System Building. *J. Chem. Inf. Model.* **2019**, *59*, 2522−2528.
(52) Abraham, M. J.; Murtola, T.; Schulz, R.; Páll, S.; Smith, J. C.; Hess, B.; Lindahl, E. GROMACS: High Performance Molecular Simulations throughMmulti-level Parallelism from Laptops to Supercomputers. *SoftwareX* **2015**, *1*−*2*, 19−25.


https://doi.org/10.1021/acs.jmedchem.1c00561
J. Med. Chem. 2021, 64, 9354−9364